Electronic Research Archive

https://www.aimspress.com/journal/era

ERA, 32(8): 4858–4886.
DOI: 10.3934/era.2024223
Received: 02 July 2024
Revised: 30 July 2024
Accepted: 05 August 2024
Published: 14 August 2024

Research article

Evolution of infectious diseases induced by epidemic prevention publicity and interaction between heterogeneous strains

Yike Lv and Xinzhu Meng*

College of Mathematics and Systems Science, Shandong University of Science and Technology, Qingdao 266590, China

* **Correspondence:** Email: mxz721106@sdust.edu.cn.

Abstract: The spread of viruses can be effectively reduced by the publicity of epidemic prevention. Additionally, the interaction between heterogeneous strains has a significant effect on virus evolution. Thus, we first establish an evolutionary dynamics Susceptible-Infected- Recovered (SIR) model which considers the interaction between heterogeneous strains. We utilize adaptive dynamics to investigate the evolutionary outcomes of the trade-off between transmission and virulence. Second, we perform a critical function analysis to generalize the results independent of specific trade-off assumptions and to determine the conditions for evolutionary stability and convergence stability. Last, we investigate the effects of different publicity measures on virulence evolution under two types of interactions, including the case of excess mortality alone and the coexistence of excess mortality and superinfection. Based on the general hypothesis of transmission virulence trade-off, we introduce the cost of host mobility caused by the scope and intensity of publicity. Numerical simulations present a set of evolutionary results, including continuously stable strategies, evolutionary branching points, repellers, and the Garden of Eden. Our results indicate that an excessive publicity scope and intensity can drive the epidemic evolution towards higher virulence. Both types of interactions suggest that continuously increasing the publicity scope under a low publicity intensity can effectively reduce virulence. Furthermore, the concurrent presence of excess mortality and superinfection induces the emergence of a higher virulence.

Keywords: SIR model; adaptive dynamics; evolutionary branching; critical function analysis; public vigilance

1. Introduction

Epidemics have always posed a serious threat to human health, prompting extensive research into epidemic diseases [1–5]. After conducting theoretical numerical simulations and analyses, epidemic models have played a crucial role in elucidating the epidemiological patterns of infectious diseases,

forecasting their changing trends, and analyzing the fundamental causes and critical factors which influence disease transmission. In studies of epidemic models, the evolutionary analysis of pathogens has become the focus of contemporary research [6–10]. These studies not only deepen our understanding of the dynamic processes in ecosystems, but also direct our focus towards early prediction and effective control strategies for virus evolution.

In studies of pathogen evolution, trade-offs reflect the constraints where a variation in one trait leads to fitness costs associated with another trait [11–13]. Many academic works have extensively studied the evolutionary outcomes of the transmission-virulence trade-off [14–17]. The implementation of epidemic prevention publicity can effectively mitigate the spread of an epidemic. However, the evolution direction of virulence can also be effected by publicity strategies. Considering the host mobility cost caused by publicity in the trade-off can explore the influence of publicity measures on virus evolution.

Different disciplines have varying definitions of the term virulence. In the theoretical study of epidemic evolution, virulence is defined as the cost of increasing the transmission of viruses [18, 19]. The trade-off theory assumes that an increase in transmission can inevitably lead to an increase in the utilization of hosts by pathogens, thus shortening the duration of infection. Therefore, virulence represents the utilization of the host. In this study, virulence represents disease-induced mortality.

Pathogens can inevitably mutate to produce variants, which are often called strains. Pathogens with multiple strains are commonly found in nature [20–22], and their evolutionary and transmission mechanisms are of significant importance in epidemiological studies. Previous studies have employed various multi-strain models to investigate this phenomenon [23–27]. This study employs an Susceptible-Infected-Recovered (SIR) model with treatment to explore the dynamic behavior of pathogens in the context of incomplete immunity after host treatment. This choice more accurately reflects the real-world scenario of diseases where a treatment does not confer immunity, thereby increasing the applicability of the model.

Meanwhile, the superinfection between hosts infected with heterogeneous strains can affect the evolution of virulence. However, there are few evolutionary studies that consider the interaction between heterogeneous strains. The result of competitive interaction usually depends on the traits that affect competitiveness [28, 29]. Therefore, by introducing interaction into the study, we can understand how competition among heterogeneous strains within the hosts influences evolution. Focusing on an SIR epidemic model, we utilize population dynamics and adaptive dynamics to investigate how varying the scope and intensity of publicity affects the evolutionary outcomes under different interactions. In additon, the critical function analysis framework is employed to study evolutionary outcomes independent of specific trade-off functions.

The rest of the paper is organized as follows. Section 2 establishes an SIR epidemic model with recovery and treatment. Then, we obtain the equilibria and discuss the conditions of global stability. In Section 3, we use population and evolutionary dynamics to study monomorphic and dimorphic populations and obtain the invasion fitness of mutant strains. Section 4 explores the relationship between the shape of trade-off and the evolutionary outcomes through a critical function analysis. In Section 5, we investigate the effect of varying the scope and intensity of publicity on virulence evolution under different interactions through a numerical simulation and analysis. Then, we conclude our paper in Section 6 with a discussion.

2. Model formulation

To investigate virus transmission among hosts, we initially analyze a Susceptible-Infected-Recovered (SIR) model in this section. We assume that all newborns are naturally susceptible, and susceptible individuals may become infected after contact with infected individuals. Additionally, our model incorporates treatment and recovery. Drug treatments can sometimes lead to a low immunity, as seen with anti-HIV and anti-influenza drugs. They control infection by inhibiting viral replication, but do not induce an immune memory against the virus. Thus, we assume that once the individuals recover, they cannot be reinfected, though infected individuals will revert to being susceptible after treatment. Therefore, we establish an epidemiological model follows:

$$\begin{cases} S'(t) = b - \beta(\alpha) S I + \delta I - dS, \\ I'(t) = \beta(\alpha) S I - (\delta + \alpha + \gamma + d) I, \\ R'(t) = \gamma I - dR, \end{cases} \tag{2.1}$$

where $S(t)$, $I(t)$, and $R(t)$ denote the sizes of susceptible, infected, and recovered individuals, respectively. Parameter b denotes the birth rate constant, and the per capita death rate is denoted by d. The parameter δ represents the treatment rate. The recovery rate is given by γ, and we assume that the hosts gain lifelong immunity once they recover. The parameter α denotes the disease-induced death rate of the infected individuals. Then, we adopt α as the measure of strain virulence to conduct the following research. The transmission rate of the strain is denoted by $\beta(\alpha)$, which depends on virulence according to the trade-off of the transmission-virulence. Since the first two terms of system (2.1) are independent of R, we only consider the following epidemic model:

$$\begin{cases} S'(t) = b - \beta(\alpha) S I + \delta I - dS, \\ I'(t) = \beta(\alpha) S I - (\delta + \alpha + \gamma + d) I. \end{cases} \tag{2.2}$$

Through simple calculations, we can determine two equilibria of system (2.2).

■ Disease-free equilibrium $E_0(S_0, I_0)$, where

$$S_0 = \frac{b}{d}, \quad I_0 = 0. \tag{2.3}$$

■ Endemic equilibrium $\hat{E}\left(\hat{S}, \hat{I}\right)$, where

$$\hat{S} = \frac{\alpha + d + \gamma + \delta}{\beta(\alpha)}, \quad \hat{I} = \frac{b\beta(\alpha) - d(\alpha + d + \gamma + \delta)}{\beta(\alpha)(\alpha + d + \gamma)}. \tag{2.4}$$

Next, we focus on the stability of the equilibria and determine the basic reproduction number of system (2.2) using the next-generation matrix [30]. The transmission scalar of system (2.2) is $F = [\beta S_0]$, and the transition scalar is $V = [\delta + \alpha + \gamma + d]$. Then, we can see that the next generation matrix is as follows:

$$NGM = FV^{-1} = \left[\frac{\beta(\alpha) S_0}{\delta + \alpha + \gamma + d}\right].$$

The maximum spectral radius is $\rho(FV^{-1}) = \frac{\beta(\alpha) S_0}{\delta + \alpha + \gamma + d}$. We can obtain the basic reproduction number as follows:

$$R_0 = \frac{\beta(\alpha) S_0}{\delta + \alpha + \gamma + d}. \tag{2.5}$$

Next, we use the basic reproduction number R_0 to determine the conditions for global stability at the two equilibria in Lemmas 2.1 and 2.2.

Lemma 2.1. *Define* $D = \left\{(S, I) | \, S \geq 0, I \geq 0, S + I \leq \frac{b}{d}\right\}$. *Region D is a positively invariant set of system* (2.2) *and is globally attractive.*

Lemma 2.2. *(i) The disease-free equilibrium point* $E_0(S_0, I_0)$ *is globally asymptotically stable when* $R_0 < 1$.

(ii) The endemic equilibrium point $\hat{E}\left(\hat{S}, \hat{I}\right)$ *is globally asymptotically stable when* $R_0 > 1$.

The detailed proofs of Lemmas 2.1 and 2.2 can be found in Appendixes A and B, respectively.

3. Adaptive dynamics

In this section, the invasive fitness of rare mutant strains is determined. Then, we explore the conditions that lead to the generation of continuously stable strategies and evolutionary branching points. We start with a monomorphic population of resident strains and then reach a dimorphic strain population. According to [31] , when a mutant strain appears, the population density of the mutant strains is assumed to be very sparse. Therefore, we ignore the effect of the mutant strain population density on the resident strain population density. Consequently, the resident strain population density of an equilibrium $\hat{E}\left(\hat{S}, \hat{I}\right)$ will affect the invasion fitness of the mutant strains.

3.1. Monomorphic adaptive dynamics

In this subsection, we examine the adaptive dynamics of a monomorphic strain population. We introduce the mutant strains I_m into system (2.2) when a small number of mutant strains with virulence α_m appear. Thus, we formulate the invasion dynamics model of system (2.2) as follows:

$$\begin{cases} S'(t) = b - \beta(\alpha) S I - \beta(\alpha_m) S I_m + \delta I + \delta I_m - dS, \\ I'(t) = \beta(\alpha) S I - (\delta + \alpha + \gamma + d) I - a(\alpha - \alpha_m) I I_m, \\ I_m'(t) = \beta(\alpha_m) S I_m - (\delta + \alpha_m + \gamma + d) I_m - a(\alpha_m - \alpha) I_m I. \end{cases} \tag{3.1}$$

Here, α_m represents the virulence of the mutant strains. I denotes the resident strain population with virulence α, and I_m indicates the mutant strain population with virulence α_m.

Meanwhile, we assume that there is an interaction between hosts infected with heterogeneous strains. a reflects the interaction resulting from differences in virulence between heterogeneous strains. This interaction aims to simulate the competition among heterogeneous strains within the host, which can lead to either an excess mortality or superinfection of the host. Virulence reflects the ability of the virus to exploit the host. Strains with a higher virulence are more competitive within the host. Conversely, strains with a lower virulence will only be suppressed within the host. Based on the above assumptions, we can conclude that the function $a(x)$ satisfies the following:

$$\text{if } x > 0, \; a(-x) > 0, \qquad a(x) + a(-x) \geq 0, \qquad a(0) = 0. \tag{3.2}$$

After a simple mathematical analysis, we find that $a'(0) \leq 0$ and $a''(0) \geq 0$. The other parameters are the same as those in system (2.2).

The population reaches an endemic equilibrium $\hat{E}\left(\hat{S},\hat{I},0\right)$ upon the appearance of rare mutant strains. Therefore, the stability of equilibrium $\hat{E}\left(\hat{S},\hat{I},0\right)$ determines whether the mutant strains can invade the resident strain population. If $\hat{E}\left(\hat{S},\hat{I},0\right)$ is stable, then the system will remain stable in the endemic equilibrium, and the mutant strains cannot invade. Conversely, if the equilibrium point is unstable, then the mutant strains can invade. We derive the Jacobian matrix of system (3.1) at $\hat{E}\left(\hat{S},\hat{I},0\right)$ as follows:

$$J_1 = \begin{bmatrix} -\beta(\alpha)\hat{I} - d & -\beta(\alpha)\hat{S} + \delta & -\beta(\alpha_m)\hat{S} + \delta \\ \beta\hat{I} & \beta\hat{S} - (\delta + \alpha + \gamma + d) & -a(\alpha - \alpha_m)\hat{I} \\ 0 & 0 & \beta(\alpha_m)S - (\delta + \alpha_m + \gamma + d) - a(\alpha_m - \alpha)I \end{bmatrix} = \begin{bmatrix} \hat{J} & J_2 \\ \mathrm{O} & J_{\mathrm{m}} \end{bmatrix},$$

where

$$\hat{J} = \begin{bmatrix} -\beta(\alpha)\hat{I} - d & -\beta(\alpha)\hat{S} + \delta \\ \beta\hat{I} & \beta\hat{S} - (\delta + \alpha + \gamma + d) \end{bmatrix}, J_2 = \begin{bmatrix} -\beta(\alpha_m)\hat{S} + \delta \\ -a(\alpha - \alpha_m)\hat{I} \end{bmatrix},$$

$$\mathrm{O} = \begin{bmatrix} 0 & 0 \end{bmatrix}, J_{\mathrm{m}} = \beta(\alpha_m)\hat{S} - (\delta + \alpha_m + \gamma + d) - a(\alpha_m - \alpha)\hat{I}.$$

It can be shown that J_1 is a block upper triangular matrix. Thus, the eigenvalues of the diagonal blocks $\hat{J}$ and J_{m} are identical to those of J_1. Lemma 2.2 demonstrates that the equilibrium point $\hat{E}\left(\hat{S},\hat{I}\right)$ is globally asymptotically stable in system (2.2) when $R_0 > 1$. We can deduce that the eigenvalues of $\hat{J}$ have negative real parts. Thus, if $J_{\mathrm{m}} < 0$, then all eigenvalues of J_1 have negative real parts, thus indicating that the equilibrium point $\hat{E}\left(\hat{S},\hat{I},0\right)$ is stable and the mutant strains can not invade. Conversely, if $J_{\mathrm{m}} > 0$, then the mutant strains can invade. Considering the properties of J_{m}, we define a function as follows:

$$S_\alpha(\alpha_m) = \beta(\alpha_m)\hat{S}(\alpha) - (\alpha_m + d + \gamma + \delta) - a(\alpha_m - \alpha)\hat{I}(\alpha), \tag{3.3}$$

where $S_\alpha(\alpha) = 0$. $S_\alpha(\alpha_m)$ represents the per capita growth rate of hosts infected with the mutant strains. If $S_\alpha(\alpha_m) > 0$, then the initial density of the mutant strains will increase, thus indicating a positive possibility of invasion by the mutant strains. Conversely, if $S_\alpha(\alpha_m) < 0$, mutant strains cannot invade. Therefore, $S_\alpha(\alpha_m)$ is called the invasion fitness [32,33], which determines whether the mutant strains can invade.

Additionally, when mutant strains are present in only a few hosts at the initial invasion stage, selectively preferred mutant strains may go extinct due to demographic stochasticity [34]. The authors of [31,35] demonstrated that the fitness gradient determines the direction of evolution, which is calculated as the partial derivative of fitness with respect to the mutant virulence. Then, we can obtain the gradient of fitness (3.3) as follows:

$$D(\alpha) = \left.\frac{\partial S_\alpha(\alpha_m)}{\partial \alpha_m}\right|_{\alpha=\alpha_m} = \beta'(\alpha)\hat{S}(\alpha) - 1 - a'(0)\hat{I}(\alpha). \tag{3.4}$$

If the fitness gradient is positive, then the mutant strains with a higher virulence can invade. Conversely, if the fitness gradient is negative, then mutant strains with a lower virulence can invade. Meanwhile, the authors of [31] indicated that α^* is called the evolutionarily singular strategy if

$$D(\alpha^*) = \left.\frac{\partial S_\alpha(\alpha_m)}{\partial \alpha_m}\right|_{\alpha=\alpha_m=\alpha^*} = \beta'(\alpha^*)\hat{S}(\alpha^*) - 1 - a'(0)\hat{I}(\alpha^*) = 0. \tag{3.5}$$

The resident strain population is constantly invaded and substituted, which leads to directional evolution [31]. We prove that when the virulence is far from the singular strategy, if $S_\alpha(\alpha_m) > 0$ and $R_0(\alpha_m) > 0$, then the mutant strain can invade and make a virulence substitution , as shown in Appendix C.

The authors of [36] demonstrated that strains with different virulence cannot coexist when competition within hosts between heterogeneous strains is not considered. From [37, 38], we understand that virulence will evolve towards minimizing $S(\alpha)$, thus indicating that it will maximize the basic reproduction number R_0. However, these conclusions are based on the assumption of a single-infection, and does not consider the competition among heterogeneous strains within the host. By substituting the basic reproduction number $R_0(\alpha) = \beta(\alpha) S_0/(\delta + \alpha + r + d)$, we can rewrite Eq (3.5) as follows:

$$D(\alpha^*) = \left.\frac{\partial S_\alpha(\alpha_m)}{\partial \alpha_m}\right|_{\alpha=\alpha_m=\alpha^*} = R_0'(\alpha^*)\frac{(\alpha^* + d + \gamma + \delta)^2}{\beta(\alpha^*)} - a'(0)\hat{I}(\alpha^*) = 0. \tag{3.6}$$

From assumption (3.2), we have $a'(0) \leq 0$. It is evident that the right-hand side of Eq (3.6) is non-negative. We can conclude that virulence will evolve towards the region where $R_0'(\alpha) < 0$, surpassing the point where $R_0(\alpha)$ is maximized. The competition among heterogeneous strains within the host favors strains with a higher virulence, thus providing them with greater fitness benefits. Virulence evolution resembles an arms race, where the selective pressure of asymmetric competition within the host drives strains to evolve towards a higher virulence.

The author of [35] suggested that the adaptive dynamics of virulence α can be approximated by the following:

$$\frac{d\alpha}{dt} = \frac{1}{2}\mu\sigma^2\hat{I}(\alpha) D(\alpha), \tag{3.7}$$

where μ denotes the probability of a virulence mutation occurring in an infected host, and σ^2 denotes the variance of the mutation distribution within a infected host. Thus, $\frac{1}{2}\mu\sigma^2$ represents the mutation rate of a strain. $\hat{I}$ is the population density of a strain at equilibrium $\hat{E}$ [31].

As a result of repeated invasion and a small mutation substitution, virulence evolves towards a zero fitness gradient. However, a singular strategy does not represent the direction of evolution. We determine the property of a singular strategy by calculating the second derivative of the intrusion fitness function. If

$$E = \left.\frac{\partial^2 S_\alpha(\alpha_m)}{\partial {\alpha_m}^2}\right|_{\alpha=\alpha_m=\alpha*} = \beta''(\alpha^*)\hat{S}(\alpha^*) - a''(0)\hat{I}(\alpha^*) < 0 \tag{3.8}$$

is satisfied, then the singular strategy α^* is called an evolutionarily stable strategy, thus indicating that mutant virulence near the singular strategy cannot invade α^*. Conversely, if $E > 0$, then the singular strategy lacks evolutionary stability. There are pairs of strains nearby α^* that can mutually invade each other's population ; hence, they co-exist if

$$M = \left.\frac{\partial^2 S_\alpha(\alpha_m)}{\partial \alpha_m \partial \alpha}\right|_{\alpha=\alpha_m=\alpha^*} = \beta'(\alpha^*)\hat{S}'(\alpha^*) - a'(0)\hat{I}'(\alpha^*) + a''(0)\hat{I}(\alpha^*) < 0 \tag{3.9}$$

is satisfied. If M is positive, then there are mutually exclusive pairs of strains, which means that neither can spread in the other's population. The singular strategy is called a convergence stable strategy if

$$\begin{aligned} E+M=&\frac{\partial^2 S_\alpha(\alpha_m)}{\partial {\alpha_m}^2}\bigg|_{\alpha=\alpha_m=\alpha*}+\frac{\partial^2 S_\alpha(\alpha_m)}{\partial\alpha_m\partial\alpha}\bigg|_{\alpha=\alpha_m=\alpha^*} \\ =&\beta''(\alpha^*)\hat{S}(\alpha^*)+\beta'(\alpha^*)\hat{S}'(\alpha^*)-a'(0)\hat{I}'(\alpha^*)<0, \end{aligned} \tag{3.10}$$

where the mutant strains will approach the singular strategy through directed evolution. It is called a repeller if the singular strategy lacks a convergence stability, thus indicating that virulence will evolve away from the singular strategy. Then, according to the positivity or negativity of E and $E+M$, we obtain the definitions of a continuous stability strategy, an evolutionary branching point, a repeller, and a Garden of Eden.

Definition 3.1. *1) When $E<0$, $E+M<0$, the singular strategy α^* is both evolutionarily stable and convergence stable. This is called a continuously stable strategy (CSS), in which evolution pushes the virulence towards α^* and stops, and the singular strategy is the end point of the evolutionary process.*

2) When $E>0$, $E+M<0$, the singular strategy α^* is convergence stable but evolutionarily unstable. The singular strategy α^* is called an evolutionary branching point, which means that the fitness reaches the minimum and any nearby mutant can invade.

3) When $E>0$, $E+M>0$, the singular strategy is called a repeller and lacks convergence stability, thus indicating that virulence will evolve away from the singular strategy.

4) When $E<0$, $E+M>0$, the singular strategy is called a Garden of Eden and lacks convergence stability. Virulence will evolve away from the singular strategy. Meanwhile, the singular strategy cannot be invaded by mutant strain.

If the singular strategy α^* is a branching point, then the monomorphic strain population will reach the fitness minimum and break into two strain populations with different virulence.

3.2. Dimorphic adaptive dynamics

Evolutionary branching points produce two populations of strains with different virulence in the initial monomorphic population. We assume there are two strain subpopulations with different virulence, namely, strains I_1 with virulence α_1 and strains I_2 with virulence α_2. In this subsection, we will study the evolution of these resident strain populations with different virulence α_1 and α_2 and investigate whether further evolutionary branching or an evolutionarily stable coexistence occurs. The evolutionary dynamics model following the coexistence strategy is similar to that of the monomorphic population, which is established as follows:

$$\begin{cases} S'(t)=b-\beta(\alpha_1)SI_1-\beta(\alpha_2)SI_2-dS+\delta(I_1+I_2), \\ {I_1}'(t)=\beta(\alpha_1)SI_1-(d+\delta+\gamma+\alpha_1)I_1-a(\alpha_1-\alpha_2)I_1I_2, \\ {I_2}'(t)=\beta(\alpha_2)SI_2-(d+\delta+\gamma+\alpha_2)I_2-a(\alpha_2-\alpha_1)I_2I_1. \end{cases} \tag{3.11}$$

Thus, there the exists equilibrium point $E_2(S^*(\alpha_1,\alpha_2), {I_1}^*(\alpha_1,\alpha_2), {I_2}^*(\alpha_1,\alpha_2))$ as follows:

$$\begin{aligned} S^*(\alpha_1,\alpha_2)&=\frac{-dD+A-\sqrt{(4(bD-C)B+(dD-A)^2)}}{2B}, \\ {I_1}^*(\alpha_1,\alpha_2)&=\frac{S^*(\alpha_1,\alpha_2)\beta(\alpha_2)-(d+\gamma+\delta+\alpha_2)}{a(\alpha_2-\alpha_1)}, \\ {I_2}^*(\alpha_1,\alpha_2)&=\frac{S^*(\alpha_1,\alpha_2)\beta(\alpha_1)-(d+\gamma+\delta+\alpha_1)}{a(\alpha_1-\alpha_2)}, \end{aligned}$$

where

$$
\begin{aligned}
A &= ((d+\gamma+\delta+\alpha_2)\,a(\alpha_1-\alpha_2)+\delta a(\alpha_2-\alpha_1))\beta(\alpha_1)+((d+\gamma+\delta+\alpha_1)\,a(\alpha_2-\alpha_1)+\delta a(\alpha_1-\alpha_2))\beta(\alpha_2),\\
B &= (a(\alpha_1-\alpha_2)+a(\alpha_2-\alpha_1))\beta(\alpha_1)\beta(\alpha_2),\\
C &= \delta a(\alpha_2-\alpha_1)(d+\gamma+\delta+\alpha_1)+\delta a(\alpha_1-\alpha_2)(d+\gamma+\delta+\alpha_2),\\
D &= a(\alpha_1-\alpha_2)\,a(\alpha_2-\alpha_1).
\end{aligned}
$$

Afterwards, it can be easily verified that when the condition

$$
\begin{cases}
4(bD-C)B+(dD-A)^2>0,\\
-dDB+AB-B\sqrt{(4(bD-C)B+(dD-A)^2)}>0,\\
a(\alpha_2-\alpha_1)(S(\alpha_1,\alpha_2)\beta(\alpha_2)-(d+\gamma+\delta+\alpha_2))>0,\\
a(\alpha_1-\alpha_2)(S(\alpha_2,\alpha_1)\beta(\alpha_1)-(d+\gamma+\delta+\alpha_1))>0,
\end{cases}
\tag{3.12}
$$

is satisfied, the equilibrium $E_2(S^*(\alpha_1,\alpha_2), I_1^*(\alpha_1,\alpha_2), I_2^*(\alpha_1,\alpha_2))$ is a strictly positive ecological equilibrium point. When system reaches $E_2(S^*(\alpha_1,\alpha_2), I_1^*(\alpha_1,\alpha_2), I_2^*(\alpha_1,\alpha_2))$, the low-density population of mutant strains with virulence α_m appears in the resident dimorphic strain population, and the system (3.11) adds a mutant strain population I_m, as follows:

$$
\begin{cases}
S'(t) = b-\beta(\alpha_1)SI_1-\beta(\alpha_2)SI_2-\beta(\alpha_m)SI_m-dS+\delta(I_1+I_2+I_m),\\
I_1'(t) = \beta(\alpha_1)SI_1-(d+\delta+\gamma+\alpha_1)I_1-a(\alpha_1-\alpha_2)I_1I_2-a(\alpha_1-\alpha_m)I_1I_m,\\
I_2'(t) = \beta(\alpha_2)SI_2-(d+\delta+\gamma+\alpha_2)I_2-a(\alpha_2-\alpha_1)I_2I_1-a(\alpha_2-\alpha_m)I_2I_m,\\
I_m'(t) = \beta(\alpha_m)SI_m-(d+\delta+\gamma+\alpha_m)I_m-a(\alpha_m-\alpha_1)I_mI_1-a(\alpha_m-\alpha_2)I_mI_2.
\end{cases}
\tag{3.13}
$$

Similar to Eq (3.3), we obtain the fitness of a rare mutant strain population with virulence α_m in the resident dimorphic population as follows:

$$
S_{\alpha_1,\alpha_2}(\alpha_m) = \beta(\alpha_m)S^*-(\alpha_m+d+\gamma+\delta)-a(\alpha_m-\alpha_1)I_1^*-a(\alpha_m-\alpha_2)I_2^*. \tag{3.14}
$$

Equation (3.14) determines whether the new mutant strain can invade the dimorphic strain population. Similarly, we find the fitness gradient of the mutant as follows:

$$
\begin{cases}
D_1(\alpha_1,\alpha_2) = \left.\frac{\partial S_{\alpha_1,\alpha_2}(\alpha_m)}{\partial\alpha_m}\right|_{\alpha_m=\alpha_1} = \beta'(\alpha_1)S^*(\alpha_1,\alpha_2)-1-a'(0)I_1^*-a'(\alpha_1-\alpha_2)I_2^*,\\
D_2(\alpha_1,\alpha_2) = \left.\frac{\partial S_{\alpha_1,\alpha_2}(\alpha_m)}{\partial\alpha_m}\right|_{\alpha_m=\alpha_2} = \beta'(\alpha_2)S^*(\alpha_1,\alpha_2)-1-a'(\alpha_2-\alpha_1)I_1^*-a'(0)I_2^*.
\end{cases}
\tag{3.15}
$$

Equation (3.15) determines the evolutionary direction of virulence. Since the mutant strains are rare and random, the adaptive dynamics of α_1 and α_2 can be indicated by the following:

$$
\begin{cases}
\frac{d\alpha_1}{dt} = \frac{1}{2}\mu_1\sigma_1^2 I_1(\alpha_1,\alpha_2)D_1(\alpha_1,\alpha_2) \triangleq m_1(\alpha_1,\alpha_2)D_1(\alpha_1,\alpha_2),\\
\frac{d\alpha_2}{dt} = \frac{1}{2}\mu_2\sigma_2^2 I_2(\alpha_1,\alpha_2)D_2(\alpha_1,\alpha_2) \triangleq m_2(\alpha_1,\alpha_2)D_2(\alpha_1,\alpha_2),
\end{cases}
\tag{3.16}
$$

where $I_i(\alpha_1,\alpha_2)$ represents the equilibrium density of the resident strain population I_i, μ_i denotes the probability of generating an individual mutation in the strain population, σ_i^2 denotes the variance of the mutation distribution of the resident strains I_1, I_2, and $m_i(\alpha_1,\alpha_2) = \frac{1}{2}\mu_i\sigma_i^2 I_i(\alpha_1,\alpha_2)$ denotes the

evolutionary rate of the resident strain population. In the following, we will discuss the conditions for generating CSS and evolutionary branching points in dimorphic strain populations. As seen in [39], the conditions for convergence stability in polymorphic populations are not straightforward. In the dimorphic strain population evolution, evolutionarily singular dimorphism is the coalition of strain population strategies, where the fitness gradient of each strategy is zero. Thus, we can obtain that

$$D_1\left({\alpha_1}^*, {\alpha_2}^*\right) = 0, \quad D_2\left({\alpha_1}^*, {\alpha_2}^*\right) = 0. \tag{3.17}$$

The evolutionarily singular dimorphism is evolutionarily stable if

$$\left.\frac{\partial^2 s_{{\alpha_1}^*,{\alpha_2}^*}(\alpha_m)}{\partial {\alpha_m}^2}\right|_{\alpha_m={\alpha_1}^*} < 0, \quad \left.\frac{\partial^2 s_{{\alpha_1}^*,{\alpha_2}^*}(\alpha_m)}{\partial {\alpha_m}^2}\right|_{\alpha_m={\alpha_2}^*} < 0. \tag{3.18}$$

By calculating Eq (3.14), we obtain that

$$\begin{cases} \left.\frac{\partial^2 S_{{\alpha_1}^*,{\alpha_2}^*}(\alpha_m)}{\partial {\alpha_m}^2}\right|_{\alpha_m={\alpha_1}^*} = \beta''\left({\alpha_1}^*\right) S^*\left({\alpha_1}^*, {\alpha_2}^*\right) - a''(0)\, {I_1}^*\left({\alpha_1}^*, {\alpha_2}^*\right) - a''\left({\alpha_1}^* - \alpha_2^*\right) {I_2}^*\left({\alpha_1}^*, {\alpha_2}^*\right), \\ \left.\frac{\partial^2 S_{{\alpha_1}^*,{\alpha_2}^*}(\alpha_m)}{\partial {\alpha_m}^2}\right|_{\alpha_m={\alpha_2}^*} = \beta''\left({\alpha_2}^*\right) S^*\left({\alpha_1}^*, {\alpha_2}^*\right) - a''\left({\alpha_1}^* - \alpha_2^*\right) {I_1}^*\left({\alpha_1}^*, {\alpha_2}^*\right) - a''(0)\, {I_2}^*\left({\alpha_1}^*, {\alpha_2}^*\right). \end{cases} \tag{3.19}$$

The locally convergence stability of the singular dimorphism $({\alpha_1}^*, {\alpha_2}^*)$ can be obtained from the eigenvalues, which can be gotten from the eigenvalues of the Jacobi matrix of system (3.16), which is as follows:

$$J^* = \left.\begin{bmatrix} m_1(\alpha_1,\alpha_2)\frac{\partial D(\alpha_1,\alpha_2)}{\partial \alpha_1} & m_1(\alpha_1,\alpha_2)\frac{\partial D(\alpha_1,\alpha_2)}{\partial \alpha_2} \\ m_2(\alpha_1,\alpha_2)\frac{\partial D(\alpha_1,\alpha_2)}{\partial \alpha_1} & m_2(\alpha_1,\alpha_2)\frac{\partial D(\alpha_1,\alpha_2)}{\partial \alpha_2} \end{bmatrix}\right|_{\substack{\alpha_1={\alpha_1}^* \\ \alpha_2={\alpha_2}^*}}. \tag{3.20}$$

The strong convergence stability of the dimorphic evolutionary dynamics is determined when the conditions $\det(J^*) > 0$, $\mathrm{tr}(J^*)$ are satisfied, which implies, in our case, that

$$\left.\frac{\partial D_i(\alpha_1,\alpha_2)}{\partial \alpha_i}\right|_{\substack{\alpha_1={\alpha_1}^* \\ \alpha_2={\alpha_2}^*}} < 0, \tag{3.21}$$

for $i = 1, 2$, and

$$\left.\left[\frac{\partial D_1(\alpha_1,\alpha_2)}{\partial \alpha_1}\frac{\partial D_2(\alpha_1,\alpha_2)}{\partial \alpha_2}\right]\right|_{\substack{\alpha_1={\alpha_1}^* \\ \alpha_2={\alpha_2}^*}} > \left.\left[\frac{\partial D_1(\alpha_1,\alpha_2)}{\partial \alpha_2}\frac{\partial D_2(\alpha_1,\alpha_2)}{\partial \alpha_1}\right]\right|_{\substack{\alpha_1={\alpha_1}^* \\ \alpha_2={\alpha_2}^*}}. \tag{3.22}$$

After that, similar to the monomorphic population, we can obtain the conditions of the evolutionary results. We assume that condition (3.12) is satisfied. For the evolutionarily singular dimorphism $({\alpha_1}^*, {\alpha_2}^*)$ of system (3.15), we can obtain the following:

■ If conditions (3.18), (3.21), and (3.22) are satisfied, then the singular dimorphism $({\alpha_1}^*, {\alpha_2}^*)$ is a continuously stable strategy.

■ If conditions (3.21) and (3.22) are satisfied and condition (3.18) is not satisfied, then the singular dimorphism $({\alpha_1}^*, {\alpha_2}^*)$ is an evolutionary branching point.

4. Critical function analysis

In this section, we employ a critical function analysis [36,40] to study the properties of evolutionary singular strategies when the transmission trade-off lacks a specific form. Equation (3.5) is satisfied once virulence reaches the singular strategy α^*. Then, we can obtain the following:

$$\beta'(\alpha^*) = \frac{1 + a'(0)\hat{I}(\alpha^*)}{\hat{S}(\alpha^*)}, \tag{4.1}$$

where $\hat{S}$ and $\hat{I}$ depend on the endemic equilibrium $\hat{E}\left(\hat{S}, \hat{I}\right)$. We obtain an ordinary differential equation as follows:

$$\beta'_{\text{crit}}(\alpha) = \frac{1 + a'(0)\hat{I}(\alpha)}{\hat{S}(\alpha)}. \tag{4.2}$$

Critical functions refer to the solutions of Eq (4.2) with varying initial values. In the α, β plane, each point will have a slope which corresponds to the critical function. If the trade-off is tangent to the critical function at a point, then from Eqs (3.5) and (4.1), it follows that the corresponding virulence at this tangent point is a singular strategy. We utilize the shape of a trade-off function at the tangent point to ascertain the properties of singular strategies.

Theorem 4.1. *We superimpose the image of the trade-off function on the critical function. If the condition* $a''(0) \geq 0$ *is satisfied and the trade-off function is concave at the tangent point, then the singular strategy is an evolutionarily stable strategy.*

Proof. By calculation, we obtain the second-order partial derivative of $S_\alpha(\alpha_m)$ with respect to α_m as follows:

$$E = \left.\frac{\partial^2 S_\alpha(\alpha_m)}{\partial {\alpha_m}^2}\right|_{\alpha=\alpha_m=\alpha*} = \beta''(\alpha^*)\hat{S}(\alpha^*) - a''(0)\hat{I}(\alpha^*) < 0.$$

From Inequality (3.8), we can get that if the conditions $a''(0) \geq 0$ and the trade-off function $\beta(\alpha)$ is concave at the tangent point are satisfied, then the evolutionarily singular strategy is evolutionarily stable. □

Theorem 4.2. *(1) If the trade-off at the tangent is less convex than the critical function, then the singular strategy is convergence stable.*

(2) When (1) is satisfied and trade-off $\beta(\alpha)$ *is sufficiently convex at the tangent point such that the singular strategy lacks evolutionary stability, the singular strategy is an evolutionary branching point.*

Proof. (i) We find the second-order derivative of the critical function at the tangent point as follows:

$$\beta''_{\text{crit}}(\alpha^*) = \frac{a'(0)\hat{I}'(\alpha^*)\hat{S}(\alpha^*) + \hat{S}'(\alpha^*)\left(1 + a'(0)\hat{I}(\alpha^*)\right)}{\left(\hat{S}(\alpha^*)\right)^2}.$$

By substituting Eq (3.5) into the above equation, we obtain the following:

$$\beta''_{\text{crit}}(\alpha^*) = \frac{a'(0)\hat{I}'(\alpha^*) - \beta'(\alpha^*)\hat{S}'(\alpha^*)}{\hat{S}(\alpha^*)}.$$

From Inequality (3.10), we know that the condition of convergence stability is as follows:

$$E + M = \beta''(\alpha^*)\hat{S}(\alpha^*) + \beta'(\alpha^*)\hat{S}'(\alpha^*) - a'(0)\hat{I}'(\alpha^*) < 0.$$

If

$$\beta''(\alpha^*) < \frac{a'(0)\hat{I}'(\alpha^*) - \beta'(\alpha^*)\hat{S}'(\alpha^*)}{\hat{S}(\alpha^*)} = \beta''_{\text{crit}}(\alpha^*)$$

is satisfied, then the singular strategy α^* is convergence stable.

(ii) We can obtain that if the trade-off function is less convex than the critical function at the tangent point, then the evolutionarily singular strategy is convergence stable. Then, if the image of the trade-off function $\beta(\alpha)$ is sufficiently convex such that the singular strategy lacks evolutionary stability, the singular strategy is an evolutionary branching point. □

Therefore, we apply Theorems 4.1 and 4.2 to analyze the evolutionary outcomes of the singular strategy by using superimposed images of the critical and trade-off functions.

5. Evolutionary analysis

This section applies the theoretical findings to an SIR model. We utilize a critical function analysis and numerical simulations to examine the evolutionary outcomes. The transmission-virulence trade-off hypothesis [41] indicates that the virulence satisfies the following:

- when the virulence is 0, the pathogen is not transmissible;
- the increase of transmission inevitably leads to higher virulence.

To investigate the rich evolutionary potential of the model, we first follow the general trade-off assumption as follows:

$$\beta(\alpha) = \frac{c_\beta \alpha}{\eta + \alpha},$$

where the transmission rate increases with the virulence and approaches a certain upper limit [42]. While several studies have documented this trade-off, empirical research that assesses the trade-off between virulence and transmission remains insufficient. Then, we incorporate the cost of host immobility caused by fear of the virus following the epidemic prevention publicity. When implementing epidemic prevention measures, the scope and intensity of publicity increases the public awareness, leading some individuals to engage in self-isolation, thereby reducing contact between susceptible individuals and infected hosts. The contact rate of the hosts who have not been exposed to the epidemic prevention publicity does not decrease. Hosts exposed to the epidemic prevention publicity will develop the fear of the virus. This fear is not only related to the intensity and effectiveness of the publicity, but also to the virulence of the virus. To simulate the variation of this fear, we introduce a monotonically decreasing function to model the decrease in the communication rate as a result to the increase in scope and the intensity of publicity. Therefore, we define the transmission trade-off as follows:

$$\beta(\alpha) = \frac{c_\beta \alpha}{\eta + \alpha}\left(1 - k + k\exp(-va)\right), \tag{5.1}$$

where the parameters c_β, η, k, and v are all positive. The fraction outside parenthesis adheres to the general hypothesis of transmission-virulence trade-off, where transmission approaches the upper limit c_β with an increasing virulence. The parameter η determines how rapidly the function $\beta(\alpha)$ rises as

α increases. Then, we use the parameters k and v in parenthesis to simulate how the transmission rate changes when the scope and intensity of publicity increases. Parameters k and v describe the effects of increasing the scope and intensity of publicity, respectively, on reducing the transmission rate $\beta(\alpha)$. The scope and intensity of publicity will reduce contacts, thereby decreasing the transmission rate. Considering that it is difficult to achieve a very high publicity range in practice, we only discuss the evolutionary results for $k \leq 0.9$. Meanwhile, an increase in the virulence will also heighten the public vigilance among populations exposed to the epidemic prevention publicity, thereby reducing the transmission rate.

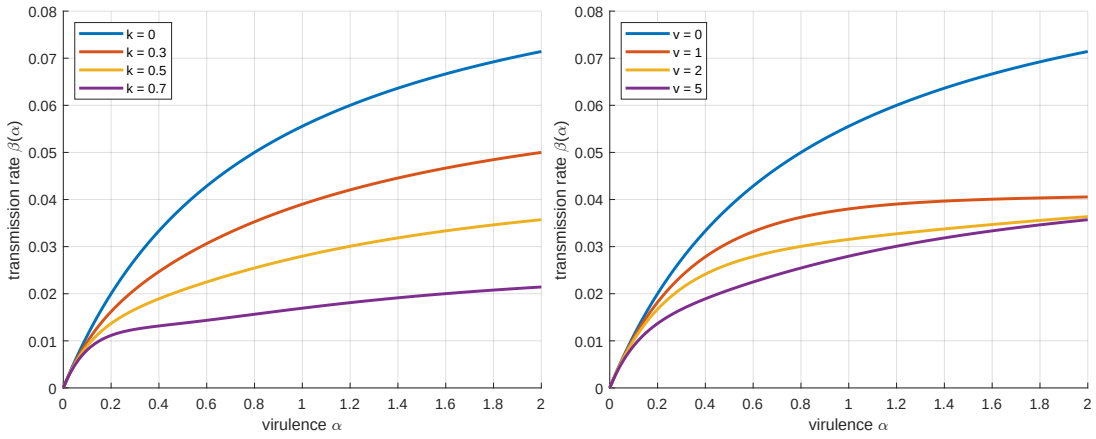

(a) $v = 5$ (b) $k = 0.5$

Figure 1. Parameter variation diagram of function given by (5.1). (a) Variation of $\beta(\alpha)$ with k when $v = 5$. Blue, red, yellow and purple represent $k = 0$, $k = 0.3$, $k = 0.5$ and $k = 0.7$ respectively. (b) Variation of $\beta(\alpha)$ with v when $k = 0.5$. Blue, red, yellow and purple represent $v = 0$, $v = 1$, $v = 2$ and $v = 5$ respectively.

Figure 1(a),(b) demonstrate that increasing the scope and intensity of publicity leads to a decrease in the transmission rate. In Figure 1(a), the scope of publicity reduces the overall transmission. The impact of the epidemic prevention publicity on individuals is influenced by both the intensity of the publicity and the severity of the outbreak. Increasing the publicity intensity and virulence amplifies public fear of the virus. Figure 1(b) shows that increasing the publicity intensity effectively reduces the transmission rate when virulence is low. However, when virulence is high, the impact of the publicity intensity on the transmission rate is not significant.

Next, we explore the impact of varying publicity measures on the evolution of virulence in diverse interactions between heterogeneous strains.

5.1. Excess mortality

In this subsection, we assume that contact with infected hosts only results in excess mortality, thus indicating that the interaction function $a(x)$ satisfies the following:

- For any x, we have $a(x) \geq 0$;
- $a(x) = 0$, if and only if $x = 0$.

By a simple mathematical analysis, we can obtain $a'(0) = 0$, $a''(0) \geq 0$. Then,we predict the

evolutionary outcomes under this interaction. The following theorem demonstrates that this interaction will not result in an evolutionary branching point.

Theorem 5.1. *System* (2.2) *does not generate evolutionary branching points when excess mortality solely occurs in the interaction.*

Proof. According to conditions (3.8) and (3.10), evolutionary branching points will occur if conditions $E > 0$ and $E + M < 0$ are satisfied. It is obvious that the emergence of evolutionary bifurcation points must satisfy the following:

$$M = \beta'(\alpha^*)\hat{S}'(\alpha^*) - a'(0)\hat{I}'(\alpha^*) + a''(0)\hat{I}(\alpha^*) < 0.$$

When the virulence evolves to an evolutionarily singular strategy, α^* satisfies condition (3.6). We can obtain that

$$\beta'(\alpha^*) = \frac{1 + a'(0)\hat{I}(\alpha^*)}{\hat{S}(\alpha^*)} = \frac{\left(1 + a'(0)\hat{I}(\alpha^*)\right)\beta(\alpha^*)}{d + \alpha^* + \gamma + \delta}.$$

From Eq (2.4), we can obtain the following:

$$\hat{S}'(\alpha^*) = \frac{\beta(\alpha^*) - \beta'(\alpha^*)(d + \alpha^* + \delta + \gamma)}{(\beta(\alpha^*))^2} = -\frac{a'(0)}{\beta(\alpha^*)}.$$

When there is only extra death in the interaction between heterogeneous strains, we obtain $a'(0) = 0$ and $a''(0) > 0$ from the above. Rewriting M, we can obtain the following:

$$\begin{aligned} M &= \beta'(\alpha^*)\hat{S}'(\alpha^*) - a'(0)\hat{I}'(\alpha^*) + a''(0)\hat{I}(\alpha^*) \\ &= a''(0)\hat{I}(\alpha^*) - a'(0)\frac{\beta'(\alpha^*)}{\beta(\alpha^*)} - a'(0)\hat{I}'(\alpha^*) \\ &= a''(0)\hat{I}(\alpha^*) > 0. \end{aligned}$$

Therefore, we can obtain that there will be no evolutionary branching points under a mutual inhibition competition. Obviously, M is positive, which means that there will be no evolutionary branching points when the interaction will only induce an excess mortality. □

According to Theorem 5.1, there is no evolutionary branching point under the hypothesis of excess mortality. However, evolutionary outcomes such as CSS and repeller may still occur. To describe the excess mortality caused by contact between infected hosts, we select the interaction function to be the following:

$$a(x) = c_a\left(\frac{1 + p}{1 + p\exp(\sigma x)} - 1\right)^2, \tag{5.2}$$

where the parameters c_a, σ, and p are all positive. It is evident that the function $a(x)$ satisfies condition (3.2) of the interaction function and the above conditions for an excess mortality. The parameter c_h governs the upper limit of the interaction function. σ represents the extent of the interaction between heterogeneous strains.

Figure 2(*a*) illustrates that the interaction increases more rapidly as σ becomes larger. Parameter p describes the disparity in the excess mortality caused by the interaction between the high and low virulence strains. In Figure 2(*b*), the excess mortality of the high virulence strains is lower than that of

the low virulence strains when $p > 1$. Conversely, when $0 < p < 1$, the excess mortality caused by the highly virulent strains is higher than that caused by the less virulent strains. We assume that hosts infected by the low virulence strain will experience a higher mortality rate when reinfected by the high virulence strain.

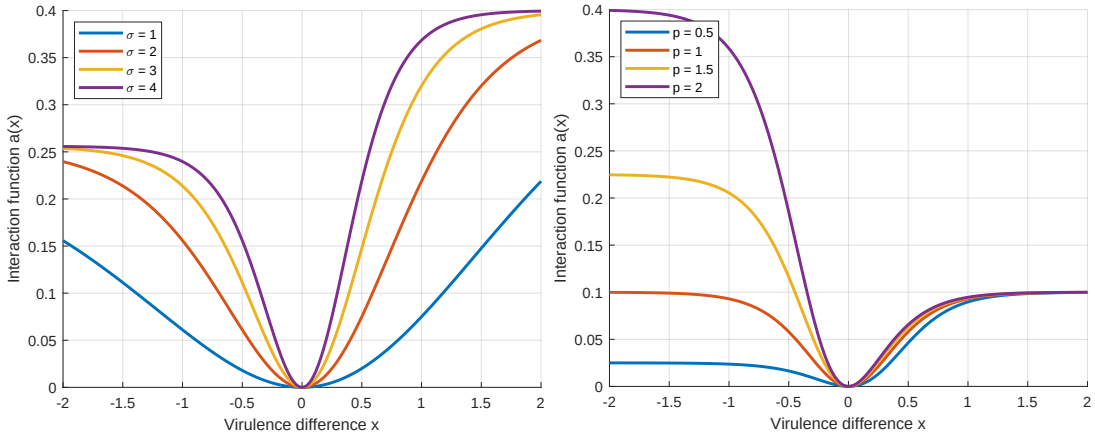

(a) $p = 0.8$ (b) $\sigma = 4$

Figure 2. Parameter variation diagram of function given by (5.2). (a) Variation of $a(x)$ with σ when $p = 0.8$. Blue, red, yellow and purple represent $\sigma = 1$, $\sigma = 2$, $\sigma = 3$, and $\sigma = 4$ respectively. (b) Variation of $a(x)$with p when $\sigma = 4$. Blue, red, yellow and purple represent $p = 0.5$, $p = 1$, $p = 1.5$, and $p = 2$ respectively.

Then, we examine the effects of various publicity measures on evolutionary outcomes when heterogeneous strains result solely in an excess mortality. Rewriting conditions (3.8) and (3.10) shows that the singular strategy is an evolutionarily stable strategy if the inequality

$$E = \beta''(\alpha^*)\hat{S}(\alpha^*) - a''(0)\hat{I}(\alpha^*) < 0 \tag{5.3}$$

is satisfied. If the inequality

$$E + M = \beta''(\alpha^*)\hat{S}(\alpha^*) < 0 \tag{5.4}$$

is satisfied, then the singular strategy is convergence stable. Evidently, the evolutionary outcomes of CSS, repeller, and the Garden of Eden may still occur.

Figure 3 illustrates the evolutionary outcomes of virulence in relation to the publicity intensity across different publicity scopes. In Figure 3(a), CSS only occurs when the publicity scope is limited, thus indicating that the virulence will stably evolve to a singular strategy. In addition, blindly increasing the publicity intensity under a limited publicity scope may not reduce the evolution direction of virulence. To mitigate virulence, we should opt for a moderate publicity intensity. Figure 3(b) depicts how the singular strategy changes with the publicity intensity as the publicity scope increases. When the publicity scope is high, increasing the publicity intensity effectively reduces the singular strategy. Continued increases in the publicity intensity can result in evolutionary bi-stability. Then, strains with an initial virulence higher than the repeller will evolve towards a high CSS. Conversely, strains with an initial virulence lower than the repeller will evolve towards a low CSS. Moreover, if the publicity intensity is further increased, then only one high CSS will exist.

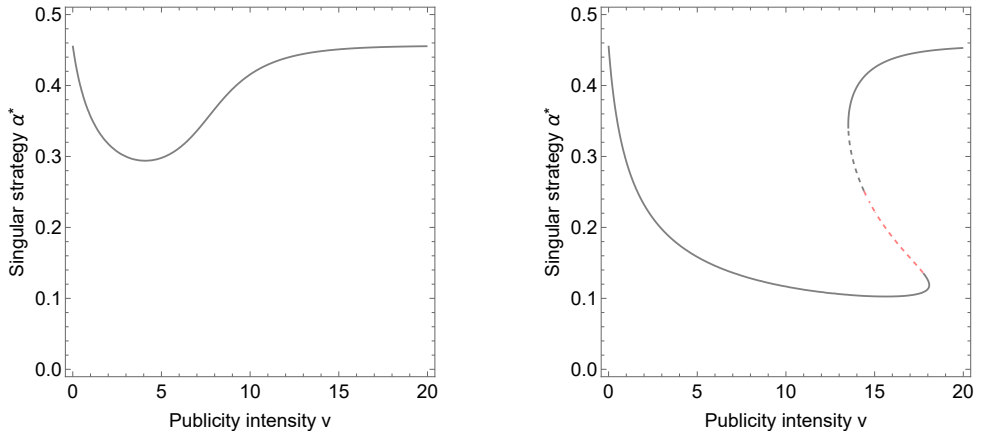

(a) k=0.4 (b) k=0.75

Figure 3. Bifurcation diagram. The red solid line indicates the evolutionary branching point, the grey solid line represents the CSS, the red dashed line denotes the repeller, and Garden of Eden is the grey dashed line. (a) Bifurcation diagram of publicity intensity with $k = 0.4$. (b) Bifurcation diagram of publicity intensity with $k = 0.75$. Nonvarying parameter values are: $c_\beta = 0.1$, $\eta = 0.8$, $c_\mathrm{a} = 0.4$, $p = 1.3$, $\sigma = 0.5$, $b = 10$, $d = 0.01$, $\gamma = 0.1$, $\delta = 0.15$.

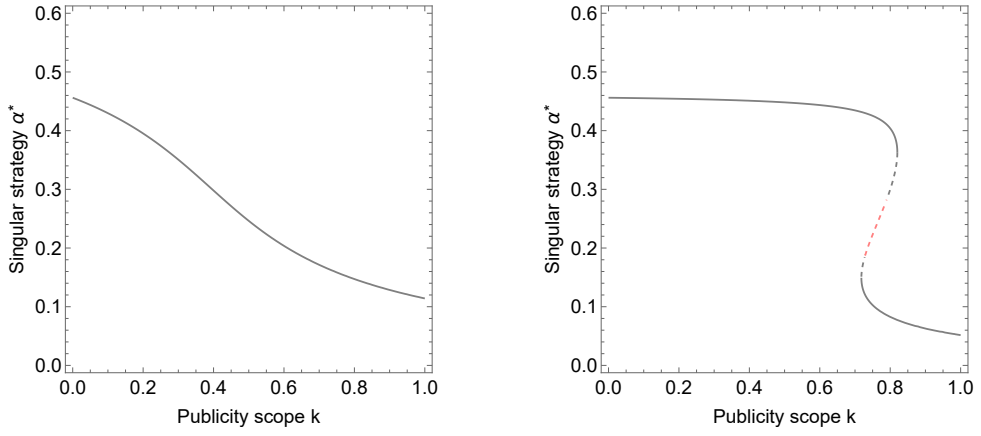

(a) v=5 (b) v=15

Figure 4. Bifurcation diagram. The line colors and styles (solid and dashed) retain the same significance as previously defined. (a) Bifurcation diagram of publicity scope with $v = 5$. (b) Bifurcation diagram of publicity scope with $v = 15$. Nonvarying parameter values are: $c_\beta = 0.1$, $\eta = 0.8$, $c_\mathrm{a} = 0.4$, $p = 1.3$, $\sigma = 0.5$, $b = 10$, $d = 0.01$, $\gamma = 0.1$, $\delta = 0.15$.

Figure 4 illustrates the effects of increasing the scope of publicity on the evolutionary direction under both a low and a high publicity intensity. In Figure 4(a), it is evident that increasing the publicity intensity only results in CSS when the publicity intensity is low. Keeping the publicity intensity low and the publicity scope high can effectively reduce the singular strategy. However, Figure 4(b) demonstrates that when the publicity intensity is high, increasing the publicity scope does not significantly reduce

the evolutionary trend of virulence. The high publicity scope will lead to an evolutionary bi-stability. Continuing to expand the publicity scope can effectively make the singular strategy only have a low CSS.

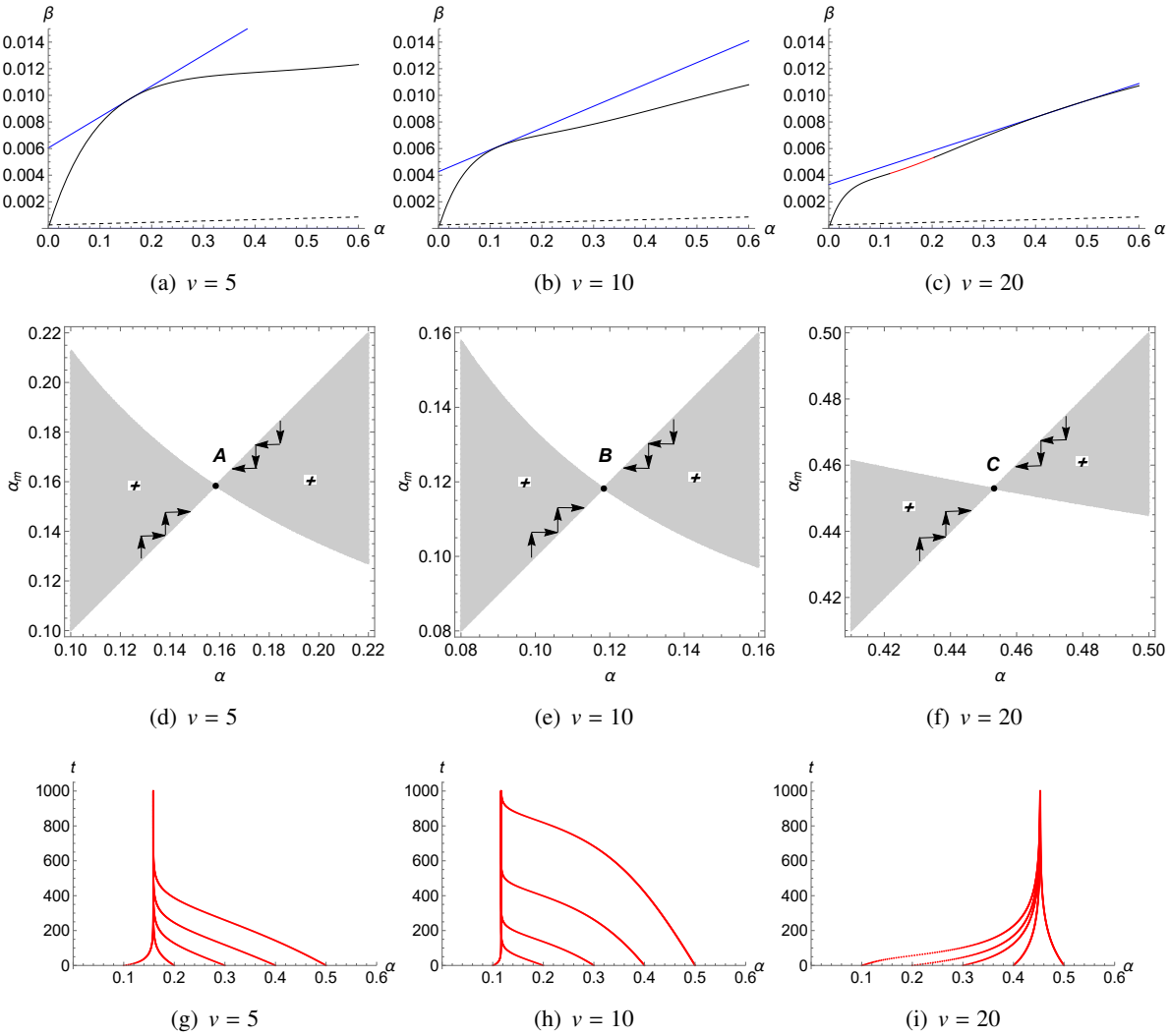

(a) $v = 5$ (b) $v = 10$ (c) $v = 20$

(d) $v = 5$ (e) $v = 10$ (f) $v = 20$

(g) $v = 5$ (h) $v = 10$ (i) $v = 20$

Figure 5. (a)–(c) Diagram for critical function analysis. The thin blue line is the critical function and the thick black line is the trade-off function. The trade-off functions of black and red represent evolutionary stability and instability, respectively. (a) The tangent point of trade-off and critical function when $v = 5$. (b) The tangent point of trade-off and critical function when $v = 10$. (c) The tangent point of trade-off and critical function when $v = 20$. (d)–(f) Pairwise invasibility plots. The mutant strains with positive fitness is indicated by the shaded area marked with '+', otherwise it is the opposite. The direction of disruptive selection which ceases at the stable strategy is indicated by '→'. (d) When $v = 5$, A is a CSS. (e) When $v = 10$, B is a CSS. (f) When $v = 20$, C is a CSS. (g)–(i) Simulated evolutionary tree. The initial virulence values are 0.1, 0.2, 0.3, 0.4 and 0.5, respectively. (g) CSS when $v = 5$. (h) CSS when $v = 10$. (i) CSS when $v = 20$. Other parameter values: $c_\beta = 0.1$, $\eta = 0.8$, $c_a = 0.4$, $p = 1.3$, $\sigma = 0.5$, $b = 10$, $d = 0.01$, $\gamma = 0.1$, $\delta = 0.15$, $k = 0.75$.

In Table 1, we list the evolutionary outcomes induced by varying the publicity measures with the interaction of excess mortality. It is evident that both an excessively strict and lax publicity measures may produce a high CSS.

Table 1. Evolutionary outcomes induced by varying publicity measures with the interaction of excess mortality.

	Low scope	High scope
Low intensity	Low CSS appears in a certain proportion	Low CSS
High intensity	Low CSS	Both low CSS, evolutionary bi-stability[1] and high CSS may appear.

[1] Evolutionary bi-stability will result in the strains with low virulence and high virulence evolve toward low CSS and high CSS, respectively.

We use a critical function analysis and the adaptive dynamics framework to investigate the effects of different publicity measures on the evolutionary outcomes. According to Theorem 4.1 and Inequality (5.4), we can deduce that the singular strategy is CSS when the transmission rate function $\beta(\alpha)$ is concave at the singular strategy. Figure 5 illustrates the evolutionary outcomes which result from different publicity intensities when a large publicity scope is chosen. From the critical function analysis, we can deduce that the singular strategies appear at the tangent points in Figure 5(a)–(c). We can clearly see that initially increasing the publicity intensity can shift the tangent point forward, thus indicating that the evolutionary direction of virulence will be reduced. However, when the publicity intensity is too high, the critical function and the trade-off function will be tangent at a high virulence. Since the trade-off function is concave at the tangent point, CSS will be generated.

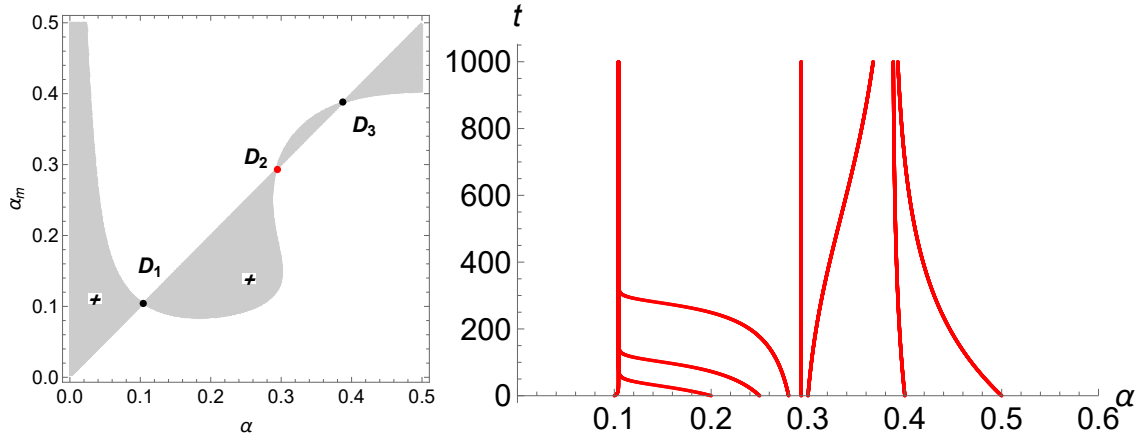

(a) $v = 13.8$ (b) $v = 13.8$

Figure 6. (a) Pairwise invasibility plot (PIP) when $v = 13.8$. '+'has the same meaning as above. D_1 and D_3 are CSS, and D_2 is a repeller. (b) Simulated evolutionary tree when $v = 13.8$. The initial virulence values are 0.1, 0.2, 0.25, 0.28, 0.29302231842516, 0.3, 0.4, and 0.5, respectively. The initial virulence of 0.29302231842516 will lead to an Garden of Eden. Other parameter values: $c_\beta = 0.1$, $\eta = 0.8$, $c_a = 0.4$, $p = 1.3$, $\sigma = 0.5$, $b = 10$, $d = 0.01$, $\gamma = 0.1$, $\delta = 0.15$, $k = 0.75$.

Figure 5(d)–(f) shows the corresponding PIP diagrams. Before reaching CSS, the virulence will

gradually evolve towards CSS. We observe that once the virulence reaches CSS, no other mutant strains can invade. Figure 5(g)–(i) is the simulated evolutionary trees. It is evident that whether the initial virulence is higher or lower than the singular strategy, it will evolve to CSS.

Meanwhile, Figure 3(c) indicates that complex evolutionary outcomes arise with a high publicity scope and intensity. Figure 6(a),(b) is pairwise invasibility plot and simulated evolutionary tree when $v = 13.8$, respectively. When evolutionary bi-stability occurs, the initial virulence smaller than the repeller D_2 will evolve to a low CSS D_1, and the initial virulence larger than the repeller D_2 will reach high CSS D_3. When the initial virulence is low, employing a high publicity scope and intensity is advisable to mitigate the strain spread. However, when faced with highly virulent strains, alternative publicity measures should be considered. Meanwhile, we observed an interesting phenomenon in Figure 6(b). Although the initial virulence near the repeller evolves towards CSS, if initial virulence happens to match the value of the repeller, then it remains unchanged. The repeller exhibits evolutionary stability, thus indicating that no mutant strain can invade. However, this scenario only exists in ideal conditions, hence it is also referred to as the Garden of Eden.

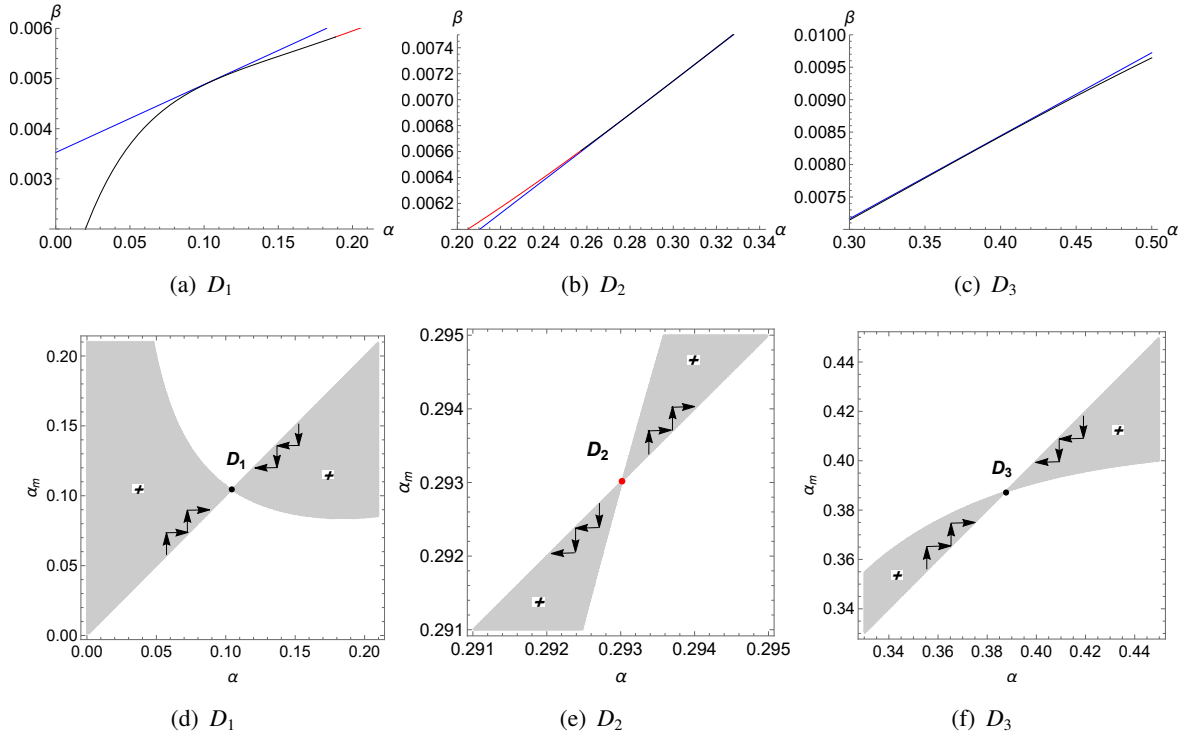

(a) D_1 (b) D_2 (c) D_3

(d) D_1 (e) D_2 (f) D_3

Figure 7. (a)–(c) Diagram for critical function analysis. The line colors and thicknesses retain the same significance as previously defined. (a) The first tangent point when $v = 13.8$. (b) The second point when $v = 13.8$. (c) The third point when $v = 13.8$. (d)–(f) Pairwise invasibility plots. '+' and '→ have the same meaning as above. (d) D_1 is a CSS. (e) D_2 is a repeller. (f) D_3 is a CSS. Other parameter values: $c_\beta = 0.1$, $\eta = 0.8$, $c_a = 0.4$, $p = 1.3$, $\sigma = 0.5$, $b = 10$, $d = 0.01$, $\gamma = 0.1$, $\delta = 0.15$, $k = 0.75$.

Figure 7(a),(c) shows that CSS will occur if $\beta(\alpha)$ is concave at the tangent point. In Figure 7(d),(f), the virulence will evolve to D_1 and D_3. When the virulence reaches D_1 and D_3, no mutant strain can

invade. According to Inequality (5.4), if the trade-off function is convex at the tangent point, then it will be convergence unstable and produce a repeller. Figure 7(b) illustrates that $\beta''(\alpha) > 0$ at the tangent point, which indicates that it is a repeller. Meanwhile, the tangent point is black, which means that the singular strategy is evolutionarily stable. Figure 7(e) shows that the virulence will leave D_2. No mutant strain can invade at D_2, which is the Garden of Eden.

5.2. *Superinfection and excess mortality*

In this section, we assume that the interaction between heterogeneous strains not only leads to excess mortality among infected individuals, but also results in superinfection. Models of super infection usually assume that the strains with a higher virulence can infect and dominate hosts that were previously infected by strains with a lower virulence [8]. Some infected hosts are taken over by strains with a higher virulence. Based on the above assumptions, we can obtain that the interaction function satisfies the following:

- If $x > 0$, $a(x) < 0$;
- $a(x) + a(-x) \geq 0$.

From Inequalities (3.8) and (3.10) and the above conditions, we observe that complex evolutionary outcomes arise under the assumptions of superinfection and an excess mortality. Meanwhile, unlike with only an excess mortality, the addition of superinfection will result in evolutionary branching. To explore the rich evolutionary outcomes under this hypothesis, we select the interaction among heterogeneous strains as follows:

$$a(x) = c_a\left(\frac{1+p}{1+p\exp(\sigma x)} - 1\right), \tag{5.5}$$

where the parameters c_a, p, and σ are all positive. The above conditions and hypothesis (3.2) regarding the interaction function are satisfied when $p \geq 1$.

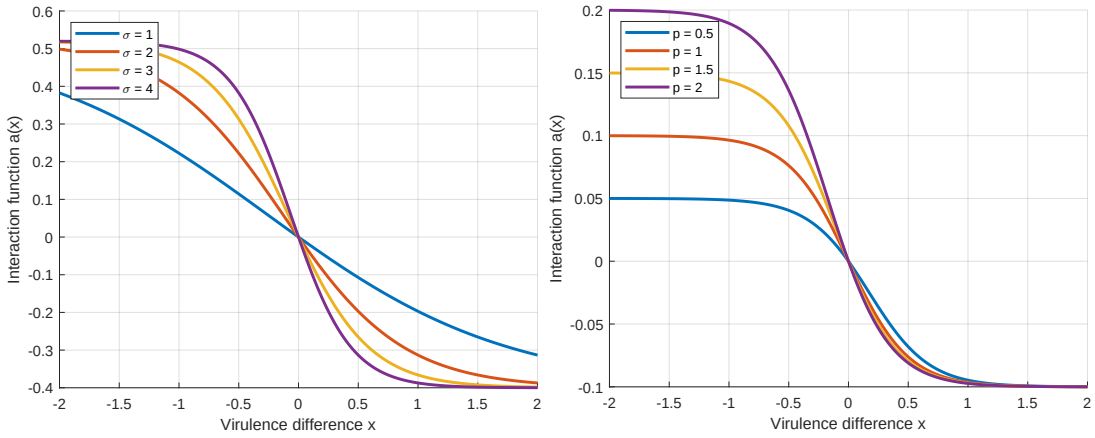

(a) $p = 1.3$ (b) $\sigma = 4$

Figure 8. Parameter variation diagram of function given by Eq (5.2). (a) Variation of $a(x)$ with σ when $p = 1.3$. Blue, red, yellow and purple represent $\sigma = 1$, $\sigma = 2$, $\sigma = 3$, and $\sigma = 4$ respectively. (b) Variation of $a(x)$ with p when $\sigma = 4$. Blue, red, yellow and purple represent $p = 0.5$, $p = 1$, $p = 1.5$ and $p = 2$ respectively.

Parameter c_a controls the upper limit of the interaction. Parameter σ describes the intensity of interaction. In Figure 8(a), as the parameter σ increases, the intensity of interaction becomes higher. p represents the proportion of superinfection and the excess mortality in the interaction. In Figure 8(b), we notice that $a(x) + a(-x)$ increases with the higher p, thus indicating a greater proportion of excess mortality. Meanwhile, when $p < 1$, $a(x) + a(-x) < 0$, which contradicts Hypothesis 3.2.

Next, we investigate the effects of various publicity measures on the evolution of virulence in the context of interactions that involve superinfection and an excess mortality.

From Eq (3.6), we can find that when $a'(0) < 0$, the interaction among heterogeneous strains will drive virulence towards a higher evolutionary direction compared to $a'(0) = 0$. Figure 9 indicates the variation of the evolutionary singular strategy with a publicity intensity in the low and high publicity scopes, respectively. Meanwhile, Figure 10 illustrates the effects of the varying publicity scopes on the direction of evolution with low and high publicity intensities. Clearly, the interaction with superinfection and an excess mortality increases the singularity strategy compared to interaction involving only the excess mortality. The rationale is that superinfection enhances the fitness benefits of strains with a higher virulence. From Figure 9(a), it is evident that at low publicity intensities, expanding the scope of publicity can effectively decrease the virulence, while also leading to evolutionary branching outcomes.

According to Figure 9(b), increasing the publicity scope at high intensity levels does not lead to a decrease in the evolutionary singularity strategies. The reduction in virulence only occurs when the publicity scope is extremely broad.

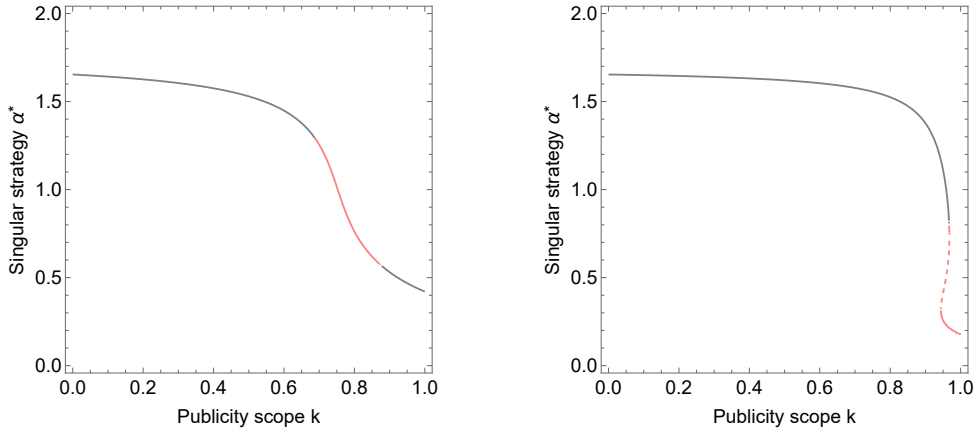

(a) v=3 (b) v=10

Figure 9. Bifurcation diagram. The line colors and styles (solid and dashed) retain the same significance as previously defined. (a) Bifurcation diagram of publicity scope with $v = 3$. (b) Bifurcation diagram of publicity scope with $v = 10$. Nonvarying parameter values are: $c_\beta = 0.1$, $\eta = 0.8$, $c_a = 0.4$, $p = 1.3$, $\sigma = 0.5$, $b = 10$, $d = 0.01$, $\gamma = 0.1$, $\delta = 0.15$.

Figure 10(a),(b) shows similar results to the interaction with only an excess mortality. Both a low and a high publicity intensity will make the singular strategy first decrease and then increase with the expansion of the scope. Meanwhile, when the publicity intensity is high, the increase of the publicity scope will produce the result of evolutionary branching.

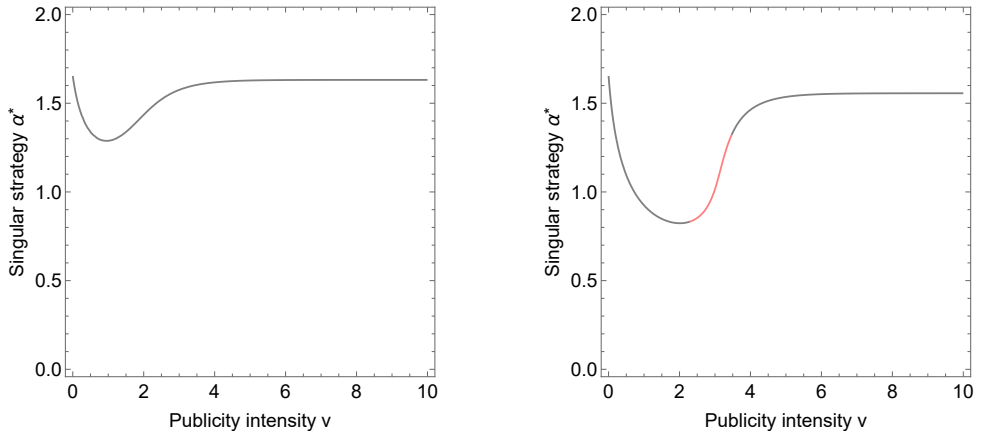

(a) k=0.4 (b) k=0.75

Figure 10. Bifurcation diagram. The line colors and styles (solid and dashed) retain the same significance as previously defined. (a) Bifurcation diagram of publicity scope under interaction 5.2 with $k = 0.4$. (b) Bifurcation diagram of publicity scope under interaction 5.2 with $k = 0.75$. Nonvarying parameter values are: $c_\beta = 0.1$, $\eta = 0.8$, $c_\mathrm{a} = 0.4$, $p = 1.3$, $\sigma = 0.5$, $b = 10$, $d = 0.01$, $\gamma = 0.1$, $\delta = 0.15$.

Table 2 list the evolutionary outcomes induced by varying the publicity measures with the interaction of an excess mortality. Different from the interaction with only excessive death, the addition of superinfection will make the evolution outcome with a high publicity intensity only a high CSS. In addition, the high range and low intensity publicity measures can produce the low CSS and evolutionary branching.

Table 2. Evolutionary outcomes induced by varying publicity measures with the interaction of Superinfection and excess mortality.

	Low scope	High scope
Low intensity	Both low CSS, evolutionary branching[1] and high CSS may appear	Both low CSS, evolutionary branching[1] and high CSS may appear
High intensity	High CSS	High CSS

[1] Evolutionary branching indicates that virulence first evolves to singular strategy, and then two strains coexist.

Next, we investigate the evolutionary outcomes that result from varying levels of publicity intensity in high publicity scopes. Figure 11 depicts critical function analyses and PIP diagrams of various publicity intensities under conditions of a high intervention scope.

Figure 11(a),(c) describe the tangents of the critical function and the trade-off function when $v = 1$ and $v = 5$. Obviously, the trade-off function at the tangent point is concave, and it is more concave than the critical function. According to Theorems 4.1 and 4.2, the tangent point is a CSS, which indicates that the singular strategy is the endpoint of evolution. Figure 11(d),(f) illustrate the corresponding PIP diagrams. We observe that virulence steadily evolves to the A and C, and no mutant strain can invade once CSS is reached. In Figure 11(d), the trade-off function is convex enough to be evolutionarily un-

stable, but not as convex as the critical function. By Theorem 4.2, evolutionary branching will appear. Figure 11(e) shows that virulence will first evolve to the evolutionary bifurcation point. After reaching the evolutionary bifurcation point B, all mutant strains with virulence near the singular strategy can invade. Then, they enter a dimorphic population where the two strains coexist.

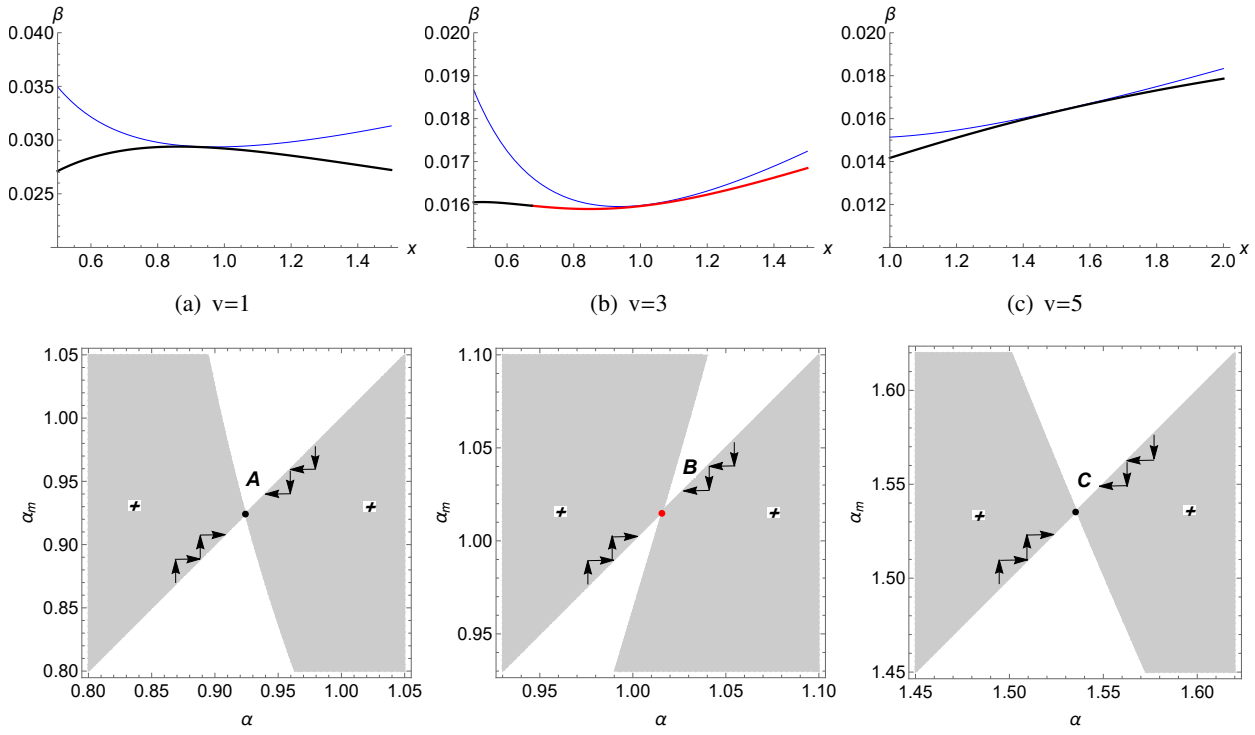

(a) v=1 (b) v=3 (c) v=5

(d) v=1 (e) v=3 (f) v=5

Figure 11. (a)–(c) Diagram for critical function analysis. The line colors and thicknesses retain the same significance as previously defined. (a) The tangent point when $v = 1$. (b) The tangent point when $v = 3$. (c) The tangent point when $v = 5$. (d)–(f) Pairwise invasibility plots. '+' and '→ have the same meaning as above. (d) A is a CSS. (e) B is an evolutionary branching point. (f) C is a CSS. Other parameter values: $c_\beta = 0.1$, $\eta = 0.8$, $c_a = 0.4$, $p = 1.3$, $\sigma = 0.5$, $b = 10$, $d = 0.01$, $\gamma = 0.1$, $\delta = 0.15$, $k = 0.75$.

Figure 12(a) indicates the virulence dynamics after entering the dimorphic population. After the virulence reaches the evolutionary branching point B, it will enter the dimorphic coexistence region. After that, the virulence dimorphism evolves into evolutionary singular dimorphisms B_1 and B_2. We can see that B_1 and B_2 meet the conditions of evolutionary stability, which indicates that they will not be invaded by other mutant strains. Figure 12(b) shows the simulated evolutionary tree with an initial virulence of 0.5. Virulence first evolves to a singular strategy, then enteres the dimorphic population and evolves to a singular dimorphism.

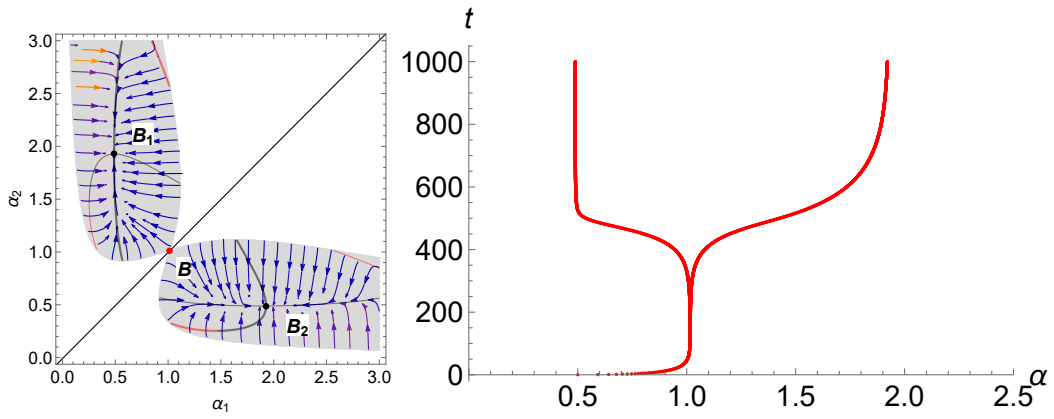

(a) Mutual invasibility plot (b) Simulated evolutionary tree

Figure 12. (a) Mutual invasibility plot. Shaded areas indicating protected dimorphism are separated by stable (black) and unstable (red) isoclines at which selection gradient vanishes in either α_1-direction (thick line) or α_2-direction (thin line). The evolutionary directions in a monomorphic environment is indicated by '$\rightarrow$' on the main diagonal. (b) Simulated evolutionary tree. Other parameter values: $c_\beta = 0.1$, $\eta = 0.8$, $c_\mathrm{a} = 0.4$, $p = 1.3$,$\sigma = 0.5$, $b = 10$, $d = 0.01$, $\gamma = 0.1$, $\delta = 0.15$, $k = 0.75$.

6. Discussion

Publicity measures for epidemic prevention have always been a common approach for humanity in combating infectious diseases. In this study, we established a fitness function to investigate the evolution of pathogens based on an SIR model. We incorporated interactions among heterogeneous strains to explore how competition within hosts effected the evolutionary outcomes. Then, we investigated the evolutionary conditions under which virulence generated CSS, evolutionary branching, repellers, and the Garden of Eden. Evolutionary outcomes independent of specific trade-offs were obtained by a critical function analysis. We followed the general hypothesis of trade-offs between transmission and virulence and incorproated the costs of host mobility induced by the scope and intensity of publicity. First, our results indicated that the introduction of interaction led a singular strategy to exceed the virulence value that maximized R_0. The interactions among heterogeneous strains induced strains with higher virulence and gained greater fitness benefits. Second, it is evident that if the interaction only involved an excess mortality, then evolutionary branching would not occur. Changing the scope and intensity of publicity led to either CSS or evolutionary bi-stability. Meanwhile, when the publicity intensity was low, a lower CSS was achieved by continuously increasing the publicity scope. However, a high publicity intensity limited the effect of the publicity scope. A high publicity scope and intensity induced the emergence of evolutionary bistability and the Garden of Eden. Third, the interaction that involved an excess mortality and superinfection drove the evolution of an increased virulence. Similar to an excess mortality, the scope of publicity reduced virulence more effectively at a low publicity intensity. Meanwhile, a high publicity scope and a low publicity intensity induced the emergence of evolutionary branching. Then, strains with different virulence will coexist. The virulence of a dimorphic population will be pushed to an evolutionarily stable singular dimorphism.

Most of the previous studies followed the trade-off that transmission increases with an increase in virulence and tends to approach an upper limit. Based on this trade-off hypothesis, we introduced the mobility cost caused by the host's fear of the virus after the epidemic prevention publicity. Therefore, we more specifically observed the effects of the epidemic prevention publicity on the virus evolution. In addition, we included the interaction between hosts infected with different strains in the model. In epidemiological research, reducing the transmission rate can effectively reduce the spread of infectious diseases. However, our results indicated that different publicity strategies induced varying evolutionary outcomes in virulence. Excessive epidemic prevention measures may result in harmful consequences. To effectively curb the spread of infectious diseases, it is imperative to thoroughly contemplate and enhance our strategies for pandemic response.

Considering the diversity of individual behaviors and the complexity of real-world epidemics, the SIR evolutionary dynamics model with treatment may not fully capture these factors. Furthermore, we investigated the evolutionary dynamics of monomorphic and polymorphic populations, since this is possible only by numerical analysis, so we provided the hypothesis of trade-off function based on biological significance and the previous research. Our conclusions are inherently tied to our hypotheses, and we aim for our assumptions to be as consistent with the empirical facts as possible. We need to take specific function forms and parameter values to simulate and verify the theoretical results of the model. Therefore, for different functions and parameters, there are certain limitations. However, the different functional assumptions may lead to similar conclusions. In the next phase of our research, we will utilize empirical data to model trade-off functions that more accurately reflect real-world dynamics.

Use of AI tools declaration

The authors declare they have not used Artificial Intelligence (AI) tools in the creation of this article.

Acknowledgments

This work is supported by the National Natural Science Foundation of China (No. 12271308) and the SDUST Innovation Fund for Graduate Students.

Conflict of interest

The authors declare there is no conflict of interest.

References

1. R. M. Anderson, R. M. May, *Infectious Diseases of Humans: Dynamics and Control*, Oxford university press, 1991.
2. X. Meng, S. Zhao, W. Zhang, Adaptive dynamics analysis of a predator–prey model with selective disturbance, *Appl. Math. Comput.*, **266** (2015), 946–958. https://doi.org/10.1016/j.amc.2015.06.020
3. H. A. Adamu, M. Muhammad, A. Jingi, M. Usman, Mathematical modelling using improved sir model with more realistic assumptions, *Int. J. Eng. Sci.*, **6** (2019), 64–69. https://doi.org/10.31873/IJEAS.6.1.22

4. H. H. Weiss, The SIR model and the foundations of public health, *Mater. Matematics*, (2013), 0001–17.
5. L. Stone, R. Olinky, A. Huppert, Seasonal dynamics of recurrent epidemics, *Nature*, **446** (2007), 533–536. https://doi.org/10.1038/nature05638
6. A. Pugliese, Evolutionary dynamics of virulence, *Elem. Adapt. Dyn.*, 2000.
7. U. Dieckmann, J. Metz, M. W. Sabelis, K. Sigmund, Adaptive dynamics of infectious diseases, *Pursuit Virulence Manage.*, (2002), 460–463. https://doi.org/10.1017/CBO9780511525728
8. B. Boldin, S. A. H. Geritz, É. Kisdi, Superinfections and adaptive dynamics of pathogen virulence revisited: a critical function analysis, *Evol. Ecol. Res.*, **11** (2009), 153–175.
9. M. Wang, J. Yi, W. Jiang, Study on the virulence evolution of sars-cov-2 and the trend of the epidemics of covid-19, *Math. Methods Appl. Sci.*, **45** (2022), 6515–6534. https://doi.org/10.1002/mma.8184
10. E. Kisdi, S. A. H. Geritz, B. Boldin, Evolution of pathogen virulence under selective predation: a construction method to find eco-evolutionary cycles, *J. Theor. Biol.*, **339** (2013), 140–150. https://doi.org/10.1016/j.jtbi.2013.05.023
11. E. L. Charnov, Phenotypic evolution under fisher's fundamental theorem of natural selection, *Heredity*, **62** (1989),, 113–116. https://doi.org/10.1038/hdy.1989.15
12. Roff, Trade-offs between growth and reproduction: an analysis of the quantitative genetic evidence, *J. Evol. Biol.*, **13** (2000), 434–445. https://doi.org/10.1046/j.1420-9101.2000.00186.x
13. S. C. Stearns, Trade-offs in life-history evolution, *Funct. Ecol.*, **3** (1989), 259–268. https://doi.org/10.2307/2389364
14. A. Pugliese, On the evolutionary coexistence of parasite strains, *Math. Biosci.*, **177** (2002), 355–375. https://doi.org/10.1016/S0025-5564(02)00083-4
15. B. Boldin, O. Diekmann, Superinfections can induce evolutionarily stable coexistence of pathogens, *J. Math. Biol.*, **56** (2008), 635–672. https://doi.org/10.1007/s00285-007-0135-1
16. S. Alizon, M. Baalen, Emergence of a convex trade-off between transmission and virulence, *Am. Nat.*, **165** (2005), E155–E167. https://doi.org/10.1086/430053
17. S. Alizon, M. Baalen, Multiple infections, immune dynamics, and the evolution of virulence, *Am. Nat.*, **172** (2008), E150–E168. https://doi.org/10.1086/590958
18. R. M. May, R. M. Anderson, Epidemiology and genetics in the coevolution of parasites and hosts, in *Proceedings of the Royal society of London. Series B. Biological sciences*, **219** (1983), 281–313. https://doi.org/10.1098/rspb.1983.0075
19. A. Best, A. White, M. Boots, The implications of coevolutionary dynamics to host-parasite interactions, *Am. Nat.*, **173** (2009), 779–791. https://doi.org/10.1086/598494
20. S. K. Sheppard, Strain wars and the evolution of opportunistic pathogens, *Curr. Opin. Microbiol.*, **67** (2022), 102138. https://doi.org/10.1016/j.mib.2022.01.009
21. A. J. Kucharski, V. Andreasen, J. R. Gog, Capturing the dynamics of pathogens with many strains, *J. Math. Biol.*, **72** (2016), 1–24. https://doi.org/10.1007/s00285-015-0873-4

22. J. R. Gog, B. T. Grenfell, Dynamics and selection of many-strain pathogens, in *Proceedings of the National Academy of Sciences*, **99** (2002), 17209–17214. https://doi.org/10.1073/pnas.252512799

23. T. Lazebnik, S. Bunimovich-Mendrazitsky, Generic approach for mathematical model of multi-strain pandemics, *PloS One*, **17** (2022), e0260683. https://doi.org/10.1371/journal.pone.0260683

24. X. Cheng, Y. Wang, G. Huang, Dynamics of a competing two-strain sis epidemic model with general infection force on complex networks, *Nonlinear Anal. Real World Appl.*, **59** (2021), 103247. https://doi.org/10.1016/j.nonrwa.2020.103247

25. I. Gordo, M. G. M. Gomes, D. G. Reis, P. R. A. Campos, Genetic diversity in the sir model of pathogen evolution, *PloS One*, **4** (2009), e4876. https://doi.org/10.1371/journal.pone.0004876

26. T. Lazebnik, Computational applications of extended sir models: A review focused on airborne pandemics, *Ecol. Modell.*, **483** (2023), 110422. https://doi.org/10.1016/j.ecolmodel.2023.110422

27. E. Numfor, N. Tuncer, M. Martcheva, Optimal control of a multi-scale hiv-opioid model, *J. Biol. Dyn.*, **18** (2024), 2317245. https://doi.org/10.1080/17513758.2024.2317245

28. S. C. Roberts, The evolution of hornedness in female ruminants, *Behaviour*, **133** (1996), 399–442. https://doi.org/10.1163/156853996X00521

29. E. Kisdi, Evolutionary branching under asymmetric competition, *J. Theor. Biol.*, **197** (1999), 149–162. https://doi.org/10.1006/jtbi.1998.0864

30. P. V. Driessche, J. Watmough, Reproduction numbers and sub-threshold endemic equilibria for compartmental models of disease transmission, *Math. Biosci.*, **180** (2002), 29–48. https://doi.org/10.1016/S0025-5564(02)00108-6

31. S. A. H. Geritz, E. Kisdi, G. M. NA, J. A. J. Metz, Evolutionarily singular strategies and the adaptive growth and branching of the evolutionary tree, *Evol. Ecol.*, **12** (1998), 35–57. https://doi.org/10.1023/A:1006554906681

32. J. A. J. Metz, R. M. Nisbet, S. A. H. Geritz, How should we define ???fitness??? for general ecological scenarios?, *Trends Ecol. Evol.*, **7** (1992), 198–202. https://doi.org/10.1016/0169-5347(92)90073-K

33. T. L. Vincent, Y. Cohen, J. S. Brown, Evolution via strategy dynamics, *Theor. Popul Biol.*, **44** (1993), 149–176. https://doi.org/10.1006/tpbi.1993.1023

34. P. Jagers, *Branching Processes with Biological Applications*, London: Wiley, 1975.

35. U. Dieckmann, R. Law, The dynamical theory of coevolution: a derivation from stochastic ecological processes, *J. Math. Biol.*, **34** (1996), 579–612. https://doi.org/10.1007/BF02409751

36. C. de Mazancourt, U. Dieckmann, Trade-off geometries and frequency-dependent selection, *Am. Nat.*, **164** (2004), 765–778. https://doi.org/10.1086/424762

37. G. Meszena, E. Kisdi, U. Dieckmann, S. A. H. Geritz, J. A. J. Metz, Evolutionary optimisation models and matrix games in the unified perspective of adaptive dynamics, *Selection*, **2** (2002), 193–220. https://doi.org/10.1556/Select.2.2001.1-2.14

38. J. Metz, S. D. Mylius, O. Diekmann, When does evolution optimise?, IIASA Interim Report, 2008.

39. C. Matessi, C. D. Pasquale, Long-term evolution of multilocus traits, *J. Math. Biol.*, **34** (1996), 613–653. https://doi.org/10.1007/BF02409752

40. É. Kisdi, Trade-off geometries and the adaptive dynamics of two co-evolving species, *Evol. Ecol. Res.*, **8** (2006), 959–973.

41. S. Alizon, A. Hurford, N. Mideo, M. Van Baalen, Virulence evolution and the trade-off hypothesis: history, current state of affairs and the future, *J. Evol. Biol.*, **22** (2009), 245–259. https://doi.org/10.1111/j.1420-9101.2008.01658.x

42. B. Boldin, E. Kisdi, On the evolutionary dynamics of pathogens with direct and environmental transmission, *Evolution*, **66** (2012), 2514–2527. https://doi.org/10.1111/j.1558-5646.2012.01613.x

Appendix

A. Proof of Lemma 2.1

When $S = 0$, we can obtain $\frac{dS}{dt} = b + \delta I > 0$. Thus, the trajectory from the positive half of the I-axis is inward to the first quadrant. When $S + I \geq \frac{b}{d}$, $\frac{d(S+I)}{dt} = b - d(S + I) - (\alpha + \gamma) I \leq -(\alpha + \gamma) I \leq 0$. We can get that $\lim_{t \to +\infty} (S + I) \leq \frac{b}{d}$. Therefore, the trajectories from the region $S + I \geq \frac{b}{d}$, $S > 0$, $I > 0$ always end up in the region D. Again, since $I = 0$ is a trajectory of the system (2.2). It follows that region D is a positive invariant set of system (2.2) and globally attractive.

B. Proof of Lemma 2.2

(1) The Jacobi matrix for the disease-free equilibrium point $E_0(S_0, I_0)$ is

$$J_0 = \begin{bmatrix} -d & -\beta S_0 + \delta \\ 0 & (\delta + \alpha + \gamma + d)(R_0 - 1) \end{bmatrix}.$$

We can see that when $R_0 < 1$, the real parts of the eigenvalues of J_0 are all negative. Then we can obtain that the disease-free equilibrium point $E_0(S_0, I_0)$ is locally asymptotically stable when $R_0 < 1$. Conversely, it is unstable when $R_0 > 1$.

To study the global stability of disease-free equilibrium point $E_0(S_0, I_0)$, we construct the Liapunov function as

$$V_0 = S - S_0 - S_0 \ln \frac{S}{S_0} + I.$$

It is clear that the function V is positive definite, and the total derivative of V with respect to t along the system (2.2) is

$$\begin{aligned} \frac{\mathrm{dV_0}}{\mathrm{dt}} &= b - dS - (\alpha + \gamma + d) I - \frac{S_0}{S}(b - \beta S I + \delta I - dS) \\ &= b - dS - (\alpha + \gamma + d) I - \frac{S_0}{S} b + \beta S_0 I - \frac{S_0}{S} \delta I + b \\ &= \left(2 - \frac{S_0}{S} - \frac{S}{S_0}\right) b + \left((R_0 - 1)(\alpha + \gamma + d + \delta) + \left(S - \frac{b}{d}\right) \frac{\delta}{S}\right) I. \end{aligned}$$

In region D, we have $S \leq \frac{b}{d}$. Then we can obtain that all parts of the above equation are non-positive when $R_0 < 1$. So $\frac{dV}{dt} \leq 0$, where $\frac{dV}{dt} = 0$ holds if and only if $S = \frac{b}{d}$, $I = 0$. Therefore, the disease-free equilibrium point $E_0(S_0, I_0)$ is globally asymptotically stable in the invariant set D. Then, we get that the disease-free equilibrium point $E_0(S_0, I_0)$ is globally asymptotically stable.

(2) The Jacobi matrix for the endemic equilibrium point $\hat{E}\left(\hat{S}, \hat{I}\right)$ is

$$\hat{J} = \begin{bmatrix} -\beta\hat{I} - d & -\beta\hat{S} + \delta \\ \beta\hat{I} & \beta\hat{S} - (\delta + \alpha + \gamma + d) \end{bmatrix}.$$

Then, the characteristic determinant of Jacobi matrix $\hat{J}$ is

$$\det\left(\lambda E - \hat{J}\right) = \begin{vmatrix} \lambda + \beta\hat{I} + d & d + \alpha + \gamma \\ -\beta\hat{I} & \lambda \end{vmatrix} = \lambda^2 + \left(\beta\hat{I} + d\right)\lambda + \beta\hat{I}(d + \alpha + \gamma),$$

where both $\beta\hat{I} + d$ and $\beta\hat{I}(d + \alpha + \delta)$ are positive when $\hat{I} = \frac{d(d+\alpha+\gamma+\delta)(R_0-1)}{\beta(d+\alpha+\gamma)} > 0$, it implies the real parts of the eigenvalues of $\hat{J}$ are negative when $R_0 > 1$. Then, we get $\hat{E}\left(\hat{S}, \hat{I}\right)$ is locally asymptotically stable when $R_0 > 1$. On the contrary, it is unstable when $R_0 < 1$. To study the global stability of endemic equilibrium point $\hat{E}\left(\hat{S}, \hat{I}\right)$, we construct the Liapunov function as

$$\hat{V} = \frac{1}{2}\left(S - \hat{S} + I - \hat{I}\right)^2 + I - \hat{I} - \hat{I}\ln\frac{I}{\hat{I}}.$$

Meanwhile, we can get that $b = d\hat{S} + (\gamma + \sigma + d)\hat{I}$ and $\gamma + \sigma + d + \delta = \beta(\alpha)\hat{S}$. It is evident that the function V is positive definite, and the total derivative of V with respect to t along the system (2.2) is

$$\begin{aligned}
\frac{\mathrm{d}\hat{\mathrm{V}}}{\mathrm{dt}} &= \left(S - \hat{S} + I - \hat{I}\right)\left(\frac{\mathrm{dS}}{\mathrm{dt}} + \frac{\mathrm{dI}}{\mathrm{dt}}\right) + \frac{\gamma + \alpha}{\beta(\alpha)}\left(1 - \frac{\hat{I}}{I}\right)\frac{\mathrm{dI}}{\mathrm{dt}} \\
&= \left(S - \hat{S} + I - \hat{I}\right)(b - dS - (\gamma + \alpha + d)I) + \frac{\gamma + \alpha}{\beta(\alpha)}\left(1 - \frac{\hat{I}}{I}\right)(\beta(\alpha)SI - (\delta + \alpha + \gamma + d)I) \\
&= d\left(S - \hat{S} + I - \hat{I}\right)\left(\hat{S} - S + \hat{I} - I\right) + (\gamma + \alpha)\left(I - \hat{I}\right)\left(\hat{I} - I\right) + (\gamma + \alpha)\left(S - \hat{S}\right)\left(\hat{I} - I\right) \\
&\quad + \frac{\gamma + \alpha}{\beta(\alpha)}\left(I - \hat{I}\right)\left(\beta(\alpha)S - \beta(\alpha)\hat{S}\right) \\
&= -d\left(S - \hat{S} + I - \hat{I}\right)^2 - (\gamma + \alpha)\left(I - \hat{I}\right)^2 \leq 0.
\end{aligned}$$

Thus, if $R_0 > 1$, we have $\frac{\mathrm{d}\hat{\mathrm{V}}}{\mathrm{dt}} \leq 0$ in R^3_+ and $\frac{\mathrm{d}\hat{\mathrm{V}}}{\mathrm{dt}} = 0$ if and only if $(S, I) = \left(\hat{S}, \hat{I}\right)$. Following the Lyapunov-LaSalle's invariance principle, the global asymptotic stability of $\hat{E}\left(\hat{S}, \hat{I}\right)$ is proved.

C. Invasion will result in virulence substitution

In the main article, we derive the invasion fitness (3.3) of monomorphic population. $S_\alpha(\alpha_m) > 0$ will cause the equilibrium point $\left(\hat{S}(\alpha), \hat{I}(\alpha), 0\right)$ to become unstable. Substitution will occur, if the equilibrium point $\left(\hat{S}(\alpha_m), 0, \hat{I}(\alpha_m)\right)$ is stable. When the diversity of virulence $|\alpha_m - \alpha|$ is small and α_m

is far from the singular strategy, we can rewrite the invasion fitness by using a Taylor expansion around $\alpha_m = \alpha$. We can get

$$S_{\alpha}(\alpha_m) = S_{\alpha}(\alpha) + \left.\frac{\partial S_{\alpha}(\alpha_m)}{\partial \alpha_m}\right|_{\alpha_m=\alpha} (\alpha_m - \alpha) + O\left((\alpha_m - \alpha)^2\right). \tag{C.1}$$

By exchanging the virulence of the mutant strain and the resident strain, we can get

$$S_{\alpha_m}(\alpha) = S_{\alpha_m}(\alpha_m) + \left.\frac{\partial S_{\alpha_m}(\alpha)}{\partial \alpha}\right|_{\alpha=\alpha_m} (\alpha - \alpha_m) + O\left((\alpha - \alpha_m)^2\right). \tag{C.2}$$

The virulence is far the from singular strategy, which indicates that $\left.\frac{\partial S_{\alpha_m}(\alpha)}{\partial \alpha}\right|_{\alpha=\alpha_m} \neq 0$. Since $S_{\alpha}(\alpha) = S_{\alpha_m}(\alpha_m) = 0$, signs of $S_{\alpha}(\alpha_m)$ and $S_{\alpha_m}(\alpha)$ are opposite when $|\alpha_m - \alpha|$ is small and α_m is far from the singular strategy. Then, we rewrite the Jacobian matrix of system (3.1) at the $\left(\hat{S}(\alpha_m), 0, \hat{I}(\alpha_m)\right)$ as

$$J_3 = \begin{bmatrix} -\beta(\alpha_m)\hat{I}(\alpha_m) - d & -\beta(\alpha)\hat{S}(\alpha_m) + \delta & -\beta(\alpha_m)\hat{S}(\alpha_m) + \delta \\ 0 & \beta(\alpha)\hat{S}(\alpha_m) - (\delta + \alpha + \gamma + d) - a(\alpha - \alpha_m)\hat{I}(\alpha_m) & 0 \\ \beta(\alpha_m)\hat{I}(\alpha_m) & -a(\alpha_m - \alpha)\hat{I}(\alpha_m) & 0 \end{bmatrix}.$$

The characteristic determinant of J_2 is

$$\begin{aligned}
&\det(\lambda E - J_3) \\
&= \begin{vmatrix} \lambda + \beta(\alpha_m)\hat{I}(\alpha_m) + d & \beta(\alpha)\hat{S}(\alpha_m) - \delta & \beta(\alpha_m)\hat{S}(\alpha_m) - \delta \\ 0 & \lambda - \left(\beta(\alpha)\hat{S}(\alpha_m) - (\delta + \alpha + \gamma + d) - a(\alpha - \alpha_m)\hat{I}(\alpha_m)\right) & 0 \\ -\beta(\alpha_m)\hat{I}(\alpha_m) & a(\alpha_m - \alpha)\hat{I}(\alpha_m) & \lambda \end{vmatrix} \\
&= (\lambda - S_{\alpha_m}(\alpha)) \begin{vmatrix} \lambda + \beta(\alpha_m)\hat{I}(\alpha_m) + d & \beta(\alpha_m)\hat{S}(\alpha_m) - \delta \\ -\beta(\alpha_m)\hat{I}(\alpha_m) & \lambda \end{vmatrix} \\
&= (\lambda - S_{\alpha_m}(\alpha))\left(\lambda^2 + \left(\beta(\alpha_m)\hat{I}(\alpha_m) + d\right)\lambda + \left(\beta(\alpha_m)\hat{S}(\alpha_m) - \delta\right)\beta(\alpha_m)\hat{I}(\alpha_m)\right).
\end{aligned}$$

From Appendix B, we know that the solution of $\det(\lambda E - J_3) = 0$ has negative real part if $S_{\alpha_m}(\alpha) < 0$ and $R_0(\alpha_m) > 1$. Meanwhile, from Eqs (C.1) and (C.2), we find that if $S_{\alpha}(\alpha_m) > 0$, $S_{\alpha_m}(\alpha) < 0$. Then, we get that $\left(\hat{S}(\alpha_m), 0, \hat{I}(\alpha_m)\right)$ is locally asymptotically stable when $S_{\alpha}(\alpha_m) > 0$ and $R_0(\alpha_m) > 1$. Therefore, if the $R_0(\alpha_m) > 1$, the diversity of virulence $|\alpha_m - \alpha|$ is small, and α_m is far from the singular strategy, successful invasion will result in virulence substitution.